Industrial Crops & Products 191 (2023) 115968

Contents lists available at ScienceDirect

Industrial Crops & Products

journal homepage: www.elsevier.com/locate/indcrop

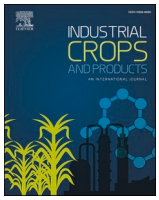

Implementation of multilayer perceptron (MLP) and radial basis function (RBF) neural networks for predicting Shatavarin IV content in Asparagus racemosus accessions.

Bibhuti Bhusan Champati [d], Bhuban Mohan Padhiari [d], Asit Ray [d], Sudipta Jena [d], Ambika Sahoo [d], Sujata Mohanty [a], Jeetendranath Patnaik [b], Pradeep Kumar Naik [c], Pratap Chandra Panda [d], Sanghamitra Nayak [d,*]

[a] Department of Biotechnology, Rama Devi Women's University, Vidya Vihar, Bhubaneswar, Odisha, India
[b] Department of Botany, S.K.C.G Autonomous College, Paralakhemundi, Odisha, India
[c] School of Life Sciences, Sambalpur University, Jyoti Vihar, Sambalpur, Odisha, India
[d] Centre for Biotechnology, Siksha 'O' Anusandhan (Deemed to be University), Bhubaneswar, Odisha, India

ARTICLE INFO

Keywords:
ANN Model
Shatavarin IV
Bioactive compounds
HPTLC
Asparagus racemosus

ABSTRACT

The principal bioactive ingredient of *Asparagus racemosus* is Shatavarin IV, a steroidal saponin found in roots with a wide range of medicinal properties. *A. racemosus* roots are used in Ayurveda system of medicine for curing a spectrum of diseases like diarrhea, nervous disorders, dysentery, dyspepsia, tumors, inflammations, neuropathy, hyperdipsia, hepatopathy, cough, hyperacidity, bronchitis and certain infectious diseases. Many of the factors influence the production and accumulation of secondary metabolites including environmental, developmental, and genetic factors. An artificial neural network (ANN) based model was developed in this study to evaluate the influence of abiotic factors (climate and soil) and to forecast a suitable site for collecting and cultivating *A. racemosus* with high Shatavarin IV concentration. The experimental dataset contains 103 *A. racemosus* accessions collected from various phytogeographical zones of Odisha. Fourteen input parameters such as soil factors (nitrogen, phosphorus, potassium, sulphur, organic carbon, pH, electrical conductivity) and climatic factors (altitude, relative humidity, UV index, average temperature, minimum temperature, maximum temperature, annual precipitation) were considered for the study. For training, testing and validation, the datasets were randomly divided into 75%, 15%, and 15%, respectively. A validated high performance thin layer chromatography (HPTLC) method was used to determine the Shatavarin IV content. The quantity of Shatavarin IV in *A. racemosus* root extracts varied from 0.010% to 0.400% on dry weight basis among 103 accessions collected from various regions of Odisha. Two ANN model algorithms namely MLP (multilayer perceptron) and RBF (radial basis function) were used for prediction and optimization of Shatavarin IV content using environmental and soil factors. The ANN model with MLP algorithm was found to be better model as compared to the RBF algorithm. The results demonstrated that an ANN-MLP architecture with a single hidden layer of 8 neurons having 14–8–1 topology could reliably predict Shatavarin IV content with a coefficient of determination (R^2) of 0.970. The prediction efficiency of the developed model was 90.740%. Sensitivity analysis revealed that nitrogen and phosphorus have a greater impact on Shatavarin IV biosynthesis than the other parameters. The content of Shatavarin IV could be increased from 0.245% to 0.300% by managing these sensitive factors in the developed model. The developed ANN model would be very useful in predicting the best regions/sites for *A. racemosus* with optimum Shatavarin IV yield.

1. Introduction

Asparagus racemosus Willd., commonly known as Shatavari is an important medicinal plant of the family Liliaceae (Goyal et al., 2003). The plant is a perennial climber and the stem grows into few meters in length. It has both fibrous and tuberous roots. It generally grows on low

* Corresponding author.
E-mail address: sanghamitran24@gmail.com (S. Nayak).

https://doi.org/10.1016/j.indcrop.2022.115968
Received 6 September 2022; Received in revised form 22 October 2022; Accepted 9 November 2022

forest areas throughout the India. The root of the plant is used as the chief ingredient in reproductive tonics due to its ability to increase the vitality in females (Joshi, 2016). The therapeutic uses of this plant have been described in the traditional system of medicines like Ayurveda, Siddha and Unani. It is one of the widely used Ayurvedic rasayana and for its wide array of aliments it is rightly called "Queen of Herbs" (Thakur et al., 2021). Traditionally it is used for the treatment of wounds, haemorrhage, urinary disorders (Arya et al., 2018). The modern research has proved various therapeutic efficacies of *A. racemosus* such as anti-diarrhoeal, antistress, antidyspepsia, antiulcerogenic action, cardio protection, antioxidant & adaptogenic properties (Mishra et al., 2013).

The phytochemical analysis of the plant shows the presence of steroidal saponins, flavonoids, alkaloids, carbohydrate, tannins and phenolic compounds. However, steroidal saponins form the major bioactive compound of *A. racemosus* (Majumdar et al., 2021). Although, the entire plant is known to have steroidal saponins but they are found more abundantly in the tuberous roots. The steroidal glycosides (Shatavarin I-IV) are the major among all the steroidal saponins. Shatavarin IV is the principal bioactive compound responsible for pharmaceutical and medicinal attributes of *A. racemosus* (Saran et al., 2020; Smita et al., 2017). Shatavarin IV possesses various pharmaceutical activities like anticancer, inhibitory activity against Core 2 GlcNAc-transferase in cell free assays and displays immunomodulation activity against specific T-dependent antigens in immunocompromised animals (Hayes et al., 2006). As the bioactivity of the plant largely depends upon the major phytoconstituent (Shatavarin IV), the quality of herbal drugs and raw materials will be assessed based on the amount of Shatavarin IV present in it. The production & accumulation of secondary metabolites are influenced by environmental factors like humidity, temperature, light intensity, minerals, water and CO_2 which can interfere strongly with the plant growth (Mishra, 2016; Yang et al., 2018). Keeping this in view, the different climatic and soil factors have been selected as study-parameters that would help to assess their impact on biosynthesis and content variation of Shatavarin IV in *A. racemosus*.

Artificial neural network is a statistical tool used for prediction and optimization purposes in various fields. It may be used to create a model that reveals the relationships between input and output data of a complex system with an inaccuracy of less than 20% of the output data, making it a high-accuracy model (Casalino et al., 2016). The ANN model is regarded as a reliable tool for identifying optimal parameters and their complex nonlinear interrelationships (Giri et al., 2011) and produce more accurate findings than traditional models (Alam and Naik, 2009). Several researchers have used ANN modeling to predict secondary metabolite levels in relation to soil and environmental parameters (Alam and Naik, 2009; Akbar et al., 2016; Akbar et al., 2018; Ray et al., 2020; Champati et al., 2022; Padhiari et al., 2022). The multilayer perceptron (MLP) and radial basis function (RBF) are two of the most commonly used algorithms in ANN model analysis. These algorithms have been used by various researchers for prediction and optimization purposes. Some of them concluded MLP as the best model algorithm (Kashaninejad et al., 2009; Zare et al., 2013; Abdi-Khanghah et al., 2018) and others concluded RBF as the best model algorithm (Yilmaz and Kaynar, 2011; Oludolapo et al., 2012). It may be due to nature and number of input parameters of the experimental dataset.

However, despite successful attempts to apply ANN model in prediction of secondary metabolites in plants, no research has been carried out on ANN model optimization and prediction of Shatavarin IV contents in *A. racemosus* from various geographical locations. Therefore, for the first time the present study was designed (i) to find out the best prediction model among ANN-RBF and ANN-MLP algorithms for prediction and optimization of Shatavarin IV, (ii) to identify the most influential environmental factor affecting the content of Shatavarin IV in *A. racemosus* by utilising ANN model, (iii) to forecast Shatavarin IV content at a new site using environmental factors and soil conditions and (iv) to optimize the Shatavarin IV content by changing the sensitive factors for high Shatavarin IV content in *A. racemosus*.

The present work on prediction and optimization of Shatavarin IV in *A. racemosus* through ANN model would solve multiple issues related to this plant like minimizing the human effort and collection pressure for identifying the elite germplasm accession in the wild. This would also prevent untargeted collection of germplasm with low Shatavarin IV content because the model could predict the suitable collection site based on climatic and soil conditions. Further, the model would be useful for determining the approximate yield of Shatavarin IV at new sites without uprooting or wastage of plant samples.

Secondly, the sensitivity analysis of the present study would help on one hand, in soil-nutrient management for developing proper cultivation practises for high yielding *Asparagus racemosus* while on the other hand would give helpful indicatives of different climatic factors and soil parameters affecting the biosynthesis of Shatavarin IV, so that the proper climatic and soil conditions for the cultivation could be set accordingly. The above mentioned dimensions have been addressed for the first time in the present study and thus bears all its novelty and significance for further research.

2. Materials and methods

2.1. Plant samples and chemical reagents

The plant samples were collected in the month of September-October 2020 at its maturity stage. The roots were taken off by carefully digging the soil near the rhizosphere region of the plants without uprooting the plant with minimum injury. The global positioning system (GPS) parameters like latitude, longitude and altitude of each location was noted on the spot with the help of a GPS device (Garmin 276 C, Garmin, Olathe, KS). About 500 g of soil samples were collected from each sample collection site. A total of 103 samples were accessed from different geographical regions of Odisha. The collected plants were authenticated by taxonomist Dr. P C Panda, Professor at Center for Biotechnology, Siksha 'O' Anusandhan (Deemed to be University), Bhubaneswar, Odisha, India and the herbarium was submitted to the same institute. The sample information was given in the Table 1.

The standard chemical of Shatavarin IV (90% purity) was procured from Natural Remedies Private Limited. The chemical structure of Shatavarin IV is given in the Fig. 1. Ethyl acetate (99.700%), Methanol (99.700%), Sulphuric acid (98%) and Water (HPLC grade) were obtained from Merk Life Science Private Limited, Mumbai, India. p-Anisaldehyde (98%) was purchased from HiMedia Laboratories Pvt. Ltd., Mumbai, India and Acetic acid glacial (100%) was purchased from Merck Specialities Private Limited, Mumbai, India. The HPTLC silica gel 60 F_{254} (10 × 20 cm) plates were procured from Merck KGaA, Darmstadt, Germany.

2.2. Quantification of Shatavarin IV

2.2.1. Plant sample and standard solution preparation

The powdered plant samples were extracted using methanol. 800 mg of powdered root sample was added to 10 ml of methanol and placed in Water bath (MS stirring water bath) at 60°C for 1 hr. It was then filtered through syringe filter of 0.220 μm pore size. The filtered solution was used in HPTLC analysis. The standard chemical of Shatavarin IV was prepared by dissolving in methanol. The Anisaldehyde-sulfuric acid reagent for derivatization was prepared by mixing p-Anisaldehyde, glacial acetic acid, methanol and sulphuric acid in the ratio of 0.5:10:85:5, v/v/v/v added in the same order

2.2.2. HPTLC instrumentation and chromatographic conditions

The HPTLC method was adopted from the study of Haldar et al. (2018) with slight modification. The chromatographic analysis was done by spotting the extracted solution of roots of *A. racemosus* and standard Shatavarin IV on pre-coated silica gel 60 F_{254} (10 ×20 cm)

Table 1
Geographic locations and habitats characteristics of *Asparagus racemosus* populations.

Code	Locality	District and State	Latitude	longitude	Voucher No.
AR-1	Nabaghanpur	Nayagargh, Odisha	20° 6′ 44.1'' N	85° 5′ 15.18'' E	1862/CBT
AR-2	Baigunia	Nayagargh, Odisha	20° 15' 31.32'' N	85° 12' 39.6'' E	1863/CBT
AR-3	Nabaghanpur	Nayagargh, Odisha	20° 6′ 44.1'' N	85° 5′ 15.18'' E	1864/CBT
AR-4	Tangi	Khordha, Odisha	19° 56' 44.34'' N	85° 27' 19.08'' E	1865/CBT
AR-5	Tangi	Khordha, Odisha	19° 56' 44.34'' N	85° 27' 19.08'' E	1866/CBT
AR-6	Tangi	Khordha, Odisha	19° 56' 44.34'' N	85° 27' 19.08'' E	1867/CBT
AR-7	Sankesh	Rayagada, Odisha	19° 11' 12.12'' N	83° 18' 48.6'' E	1868/CBT
AR-8	Sibapadar	Rayagada, Odisha	19° 42' 15.984'' N	83° 27' 52.56'' E	1869/CBT
AR-9	Therubali	Rayagada, Odisha	19° 17' 56.904'' N	83° 26' 29.76'' E	1870/CBT
AR-10	Therubali	Rayagada, Odisha	19° 26' 44.34'' N	83° 27' 19.08'' E	1871/CBT
AR-11	Sibapadar	Rayagada, Odisha	19° 43' 43.68'' N	83° 29' 13.2'' E	1872/CBT
AR-12	Budisila	Gajapati, Odisha	19° 7′ 45.12'' N	84° 8′ 0.6'' E	1873/CBT
AR-13	Budisila	Gajapati, Odisha	19° 7′ 45.12'' N	84° 8′ 0.6'' E	1874/CBT
AR-14	Budisila	Gajapati, Odisha	19° 7′ 45.12'' N	84° 8′ 0.6'' E	1875/CBT
AR-15	Patrabasa	Gajapati, Odisha	19° 9′ 40.608'' N	84° 14' 52.08'' E	1876/CBT
AR-16	Mahendragiri	Gajapati, Odisha	18° 58' 16.32'' N	84° 21' 12.24'' E	1877/CBT
AR-17	Mahendragiri	Gajapati, Odisha	18° 58' 20.64'' N	84° 21' 12.6'' E	1878/CBT
AR-18	Mahendragiri	Gajapati, Odisha	18° 58' 18.84'' N	84° 21' 10.8'' E	1879/CBT
AR-19	Badamasingha	Gajapati, Odisha	18° 57' 6.12'' N	84° 20' 47.4'' E	1880/CBT
AR-20	Badamasingha	Gajapati, Odisha	18° 56' 34.08'' N	84° 20' 27.24'' E	1881/CBT
AR-21	Kainpur	Gajapati, Odisha	18° 56' 19.68'' N	84° 17' 40.2'' E	1882/CBT
AR-22	Ramagiri	Gajapati, Odisha	19° 5′ 33'' N	84° 16' 30.36'' E	1883/CBT
AR-23	Ramagiri	Gajapati, Odisha	19° 5′ 32.28'' N	84° 16' 26.4'' E	1884/CBT
AR-24	Ramagiri	Gajapati, Odisha	19° 5′ 33.072'' N	84° 16' 26.04'' E	1885/CBT
AR-25	Ramagiri	Gajapati, Odisha	19° 5′ 33.18'' N	84° 16' 24.6'' E	1886/CBT
AR-26	Gandahati	Gajapati, Odisha	18° 52' 17.04'' N	84° 12' 26.64'' E	1887/CBT
AR-27	Gandahati	Gajapati, Odisha	18° 52' 6.96'' N	84° 13' 29.64'' E	1888/CBT
AR-28	Guma	Gajapati, Odisha	18° 51' 40.32'' N	84° 2′ 39.84'' E	1889/CBT
AR-29	Guma	Gajapati, Odisha	18° 56' 48.84'' N	84° 1′ 24.6'' E	1890/CBT
AR-30	Guma	Gajapati, Odisha	18° 56' 48.84'' N	84° 1′ 24.6'' E	1891/CBT
AR-31	Guma	Gajapati, Odisha	18° 56' 48.84'' N	84° 1′ 24.6'' E	1892/CBT
AR-32	Kamakhyanagar	Dhenkanal, Odisha	20° 40' 47.604'' N	85° 43' 25.932'' E	1893/CBT
AR-33	Kamakhyanagar	Dhenkanal, Odisha	20° 40' 15.204'' N	85° 43' 25.932'' E	1894/CBT
AR-34	Kamakhyanagar	Dhenkanal, Odisha	20° 40' 15.204'' N	85° 43' 25.932'' E	1895/CBT
AR-35	Tarava	Angul, Odisha	20° 42' 5.112'' N	84° 51' 13.896'' E	1896/CBT
AR-36	Tarava	Angul, Odisha	20° 42' 5.112'' N	84° 51' 13.896'' E	1897/CBT
AR-37	Purunakot	Angul, Odisha	20° 38' 29.184'' N	84° 51' 53.46'' E	1898/CBT
AR-38	Purunakot	Angul, Odisha	20° 38' 29.184'' N	84° 51' 53.46'' E	1899/CBT
AR-39	Purunakot	Angul, Odisha	20° 38' 29.184'' N	84° 51' 53.46'' E	1900/CBT
AR-40	Balukhanda Area	Puri, Odisha	19° 51' 29.88'' N	86° 2′ 27.6'' E	1901/CBT
AR-41	Balukhanda Area	Puri, Odisha	19° 51' 29.88'' N	86° 2′ 27.6'' E	1902/CBT
AR-42	Balukhanda Area	Puri, Odisha	19° 51' 27'' N	86° 2′ 11.76'' E	1903/CBT
AR-43	Balukhanda Area	Puri, Odisha	19° 51' 27'' N	86° 2′ 11.76'' E	1904/CBT
AR-44	Balukhanda Area	Puri, Odisha	19° 51' 21.96'' N	86° 2′ 11.4'' E	1905/CBT
AR-45	Balukhanda Area	Puri, Odisha	19° 51' 21.96'' N	86° 2′ 11.4'' E	1906/CBT
AR-46	Balukhanda Area	Puri, Odisha	19° 51' 27'' N	86° 2′ 11.76'' E	1907/CBT
AR-47	Sidhamatha hill area	Keonjhar, Odisha	21° 37' 5.808'' N	85° 34' 16.68'' E	1908/CBT
AR-48	Sidhamatha hill area	Keonjhar, Odisha	21° 37' 6.744'' N	85° 34' 15.6'' E	1909/CBT
AR-49	Sidhamatha hill area	Keonjhar, Odisha	21° 37' 7.068'' N	85° 34' 15.24'' E	1910/CBT
AR-50	Sidhamatha hill area	Keonjhar, Odisha	21° 37' 7.284'' N	85° 34' 14.88'' E	1911/CBT
AR-51	Sidhamatha hill area	Keonjhar, Odisha	21° 37' 6.132'' N	85° 34' 16.68'' E	1912/CBT
AR-52	Badaghagra hill sides	Keonjhar, Odisha	21° 36' 59.328'' N	85° 33' 8.64'' E	1913/CBT
AR-53	Badaghagra hill sides	Keonjhar, Odisha	21° 37' 31.944'' N	85° 33' 5.76'' E	1914/CBT
AR-54	Badaghagra hill sides	Keonjhar, Odisha	21° 37' 20.892'' N	85° 33' 3.24'' E	1915/CBT
AR-55	Badaghagra hill sides	Keonjhar, Odisha	21° 37' 20.964'' N	85° 33' 3.24'' E	1916/CBT
AR-56	Badaghagra hill sides	Keonjhar, Odisha	21° 37' 20.136'' N	85° 33' 2.52'' E	1917/CBT
AR-57	Badaghagra hill sides	Keonjhar, Odisha	21° 37' 20.028'' N	85° 33' 2.88'' E	1918/CBT
AR-58	Gonasika hill area	Keonjhar, Odisha	21° 31' 42.888'' N	85° 30' 37.8'' E	1919/CBT
AR-59	Gonasika hill area	Keonjhar, Odisha	21° 31' 41.88'' N	85° 30' 38.52'' E	1920/CBT
AR-60	Mahapadasala	Keonjhar, Odisha	21° 13' 35.4'' N	86° 15' 19.44'' E	1921/CBT
AR-61	Tagamana nala	Keonjhar, Odisha	21° 14' 33.72'' N	86° 14' 55.68'' E	1922/CBT
AR-62	Belachuti	Keonjhar, Odisha	21° 14' 41.28'' N	86° 15' 2.88'' E	1923/CBT
AR-63	Bahali	Cuttack, Odisha	20° 29' 36.24'' N	85° 10' 22.08'' E	1924/CBT
AR-64	Bahali	Cuttack, Odisha	20° 29' 36.24'' N	85° 10' 22.08'' E	1925/CBT
AR-65	Bahali	Cuttack, Odisha	20° 29' 36.24'' N	85° 10' 22.08'' E	1926/CBT
AR-66	Patrabhaga	Cuttack, Odisha	20° 30' 38.52'' N	85° 9′ 20.52'' E	1927/CBT
AR-67	Patrabhaga	Cuttack, Odisha	20° 30' 38.52'' N	85° 9′ 20.52'' E	1928/CBT
AR-68	Patrabhaga	Cuttack, Odisha	20° 30' 38.52'' N	85° 9′ 20.52'' E	1929/CBT
AR-69	Kandhabadabhuin	Cuttack, Odisha	20° 30' 11.88'' N	85° 9′ 57.6'' E	1930/CBT
AR-70	Kandhabadabhuin	Cuttack, Odisha	20° 30' 11.88'' N	85° 9′ 57.6'' E	1931/CBT
AR-71	Kandhabadabhuin	Cuttack, Odisha	20° 30' 11.88'' N	85° 9′ 57.6'' E	1932/CBT
AR-72	Jemadeipur	Cuttack, Odisha	20° 29' 51.72'' N	85° 9′ 52.2'' E	1933/CBT
AR-73	Jemadeipur	Cuttack, Odisha	20° 29' 51.72'' N	85° 9′ 52.2'' E	1934/CBT
AR-74	Jemadeipur	Cuttack, Odisha	20° 29' 51.72'' N	85° 9′ 52.2'' E	1935/CBT

(*continued on next page*)

Table 1 (*continued*)

Code	Locality	District and State	Latitude	longitude	Voucher No.
AR-75	Khajuria	Cuttack, Odisha	20° 29' 9.24'' N	85° 9′ 45.72'' E	1936/CBT
AR-76	Khajuria	Cuttack, Odisha	20° 29' 9.24'' N	85° 9′ 45.72'' E	1937/CBT
AR-77	Khajuria	Cuttack, Odisha	20° 29' 9.24'' N	85° 9′ 45.72'' E	1938/CBT
AR-78	Purukutia	Cuttack, Odisha	20° 29' 0.24'' N	85° 10' 50.52'' E	1939/CBT
AR-79	Purukutia	Cuttack, Odisha	20° 29' 0.24'' N	85° 10' 50.52'' E	1940/CBT
AR-80	Purukutia	Cuttack, Odisha	20° 29' 0.24'' N	85° 10' 50.52'' E	1941/CBT
AR-81	Purukutia	Cuttack, Odisha	20° 29' 0.24'' N	85° 10' 50.52'' E	1942/CBT
AR-82	Panchu pandav hills	Bargargh, Odisha	20° 53' 33.36'' N	82° 49' 54.12'' E	1943/CBT
AR-83	Panchu pandav hills	Bargargh, Odisha	20° 53' 33.36'' N	82° 49' 54.12'' E	1944/CBT
AR-84	Panchu pandav hills	Bargargh, Odisha	20° 53' 38.76'' N	82° 49' 48.72'' E	1945/CBT
AR-85	Nrusinghanath	Bargargh, Odisha	20° 53' 58.92'' N	82° 49' 4.44'' E	1946/CBT
AR-86	Nrusinghanath	Bargargh, Odisha	20° 53' 45.6'' N	82° 48' 49.68'' E	1947/CBT
AR-87	Nrusinghanath	Bargargh, Odisha	20° 53' 45.6'' N	82° 48' 49.68'' E	1948/CBT
AR-88	Nrusinghanath	Bargargh, Odisha	20° 53' 47.04'' N	82° 48' 48.24'' E	1949/CBT
AR-89	Nrusinghanath	Bargargh, Odisha	20° 53' 43.08'' N	82° 48' 43.2'' E	1950/CBT
AR-90	Gorunda	Bargargh, Odisha	20° 53' 53.16'' N	82° 48' 32.76'' E	1951/CBT
AR-91	Zero point	Sambalpur, Odisha	21° 29' 42.36'' N	83° 51' 11.52'' E	1952/CBT
AR-92	Debrigargh	Sambalpur, Odisha	21° 29' 57.12'' N	83° 46' 15.6'' E	1953/CBT
AR-93	Debrigargh	Sambalpur, Odisha	21° 29' 56.04'' N	83° 46' 20.28'' E	1954/CBT
AR-94	Debrigargh	Sambalpur, Odisha	21° 29' 56.04'' N	83° 46' 20.28'' E	1955/CBT
AR-95	Debrigargh	Sambalpur, Odisha	21° 29' 56.04'' N	83° 46' 20.28'' E	1956/CBT
AR-96	Karanjia	Mayurbhanj, Odisha	21° 37' 29.64'' N	86° 6′ 59.4'' E	1957/CBT
AR-97	Similipala BR*	Mayurbhanj, Odisha	21° 59' 6.36'' N	86° 17' 32.64'' E	1958/CBT
AR-98	Similipala BR*	Mayurbhanj, Odisha	21° 58' 13.44'' N	86° 20' 21.48'' E	1959/CBT
AR-99	Similipala BR*	Mayurbhanj, Odisha	21° 58' 13.8'' N	86° 20' 24.36'' E	1960/CBT
AR-100	Similipala BR*	Mayurbhanj, Odisha	21° 58' 13.8'' N	86° 22' 28.2'' E	1961/CBT
AR-101	Narayani Khola	Ganjam, Odisha	19° 41' 52.44'' N	85° 9′ 13.32'' E	1962/CBT
AR-102	Narayani Khola	Ganjam, Odisha	19° 41' 52.44'' N	85° 9′ 13.32'' E	1963/CBT
AR-103	Narayani Khola	Ganjam, Odisha	19° 41' 52.44'' N	85° 9′ 13.32'' E	1964/CBT

AR-Asparagus racemosus, *Biosphere reserve.

HPTLC plates. The samples and standards were applied to the plates by the help of CAMAG Linomat V sample applicator and a 100 ml syringe. The application volume of standard and sample were set at 2 μl/band and 6 μl/band respectively. The band length was set at 8 mm and the nitrogen gas flow was maintained at 25 kPa using nitrogen gas aspirator. The separation between the bands was set as 12 mm. The linear ascending plate development was done in mobile phase of ethyl acetate-methanol-water (7.5:1.5:1, v/v/v) using twin-trough glass chamber (CAMAG) saturated for 20 min in mobile phase at room temperature. The volume of mobile phase used was 20 ml and the run distance of mobile phase on the plate was set to 90 mm. The developed plate was then air dried with the help of an hair-dryer. The plates were visualized in a CAMAG UV cabinet at 254 nm and 366 nm light. Then, it was derivatized by dipping the plate in anisaldehyde-sulfuric acid reagent and subsequent heating at 110 °C for 5 min in hot-air oven. The plates were then viewed at 366 nm in CAMAG UV cabinet and the photos were taken in the fluorescence light after derivatization. The plate was scanned using CAMAG TLC scanner 4 equipped with winCATS Software. The scanning was done at 425 nm and the amount of Shatavarin IV present in the samples was quantified. The spectra matching was carried out in sample and standard by taking the absorbance of Shatavarin IV between 300 and 700 nm.

2.2.3. Quantitative estimation of Shatavarin IV

The calibration curve was done by plotting six different concentrations of Shatavarin IV. The Shatavarin IV was quantified by identifying the retardation factor (R_f) and comparing the spectra of the corresponding band with the standard Shatavarin IV band on the HPTLC plate. It was quantified using the calibration curve i.e., $y = c + mx$.

The method validation of quantitative analysis was carried out for linearity, limits of detection (LOD) and quantification (LOQ), precision, stability, repeatability and recovery test as per the guidelines set by International Conference on Harmonization (ICH., 2005).

Then, limit of detection (LOD) and quantification (LOQ) was calculated by using the signal to noise ratio (S/N) with the following formula.

$$LOQ = \frac{S}{N} \times 10$$

$$LOD = \frac{S}{N} \times 3.3$$

The precision was determined by injecting the replicate solution of standard for three times within a day. The stability of the standard was determined by injecting the same solution of standard for three consecutive days (0, 24, 48, 72 hr). Repeatability of compound was determined by independently preparing three replicates of reference standard solution. The recovery test was determined by the method of standard addition, which was done by adding known amount of standard to the analysed sample and then reanalysing.

2.3. Quantitative analysis of soil and climatic factors

The soil was taken at the rhizosphere at a depth of 0.5–1 m. Zip-lock polythene bags were used to collect the samples. Each site yielded around 500 gm of soil. Organic carbon (OC), nitrogen, phosphorous, potassium, and sulphur were all quantified and documented appropriately in the soil samples. The pH and electrical conductivity (EC) of the solution were also measured. The Table 2 contained all of the soil parameters.

The soil samples were sieved through a 2 mm screen and then subjected to a variety of tests. The pH of the soil samples was determined using a pH meter (Systronics, Model MKVI). Water was used to suspend the soil samples (1:2, soil:water). The pH was determined after the solution was equilibrated by regularly mixing for around 25–30 mins. The quantity of nitrogen in the soil samples was estimated using the alkaline $KMnO_4$ technique (Subbiah and Asija, 1956). 20 g of soil and 100 ml of 0.320% $KMnO_4$ solution were placed in an 800 ml Kjeldahl flask. Some distilled water was added to the 2.500% NaOH solution. The combination was then distilled, with the distillate collected in a 250 ml conical flask containing 20 ml boric acid and a mixed indicator. After that, the distillate was titrated against 0.02 N H_2SO_4 to determine the amount of accessible nitrogen. A calibration curve of standard phosphorus was

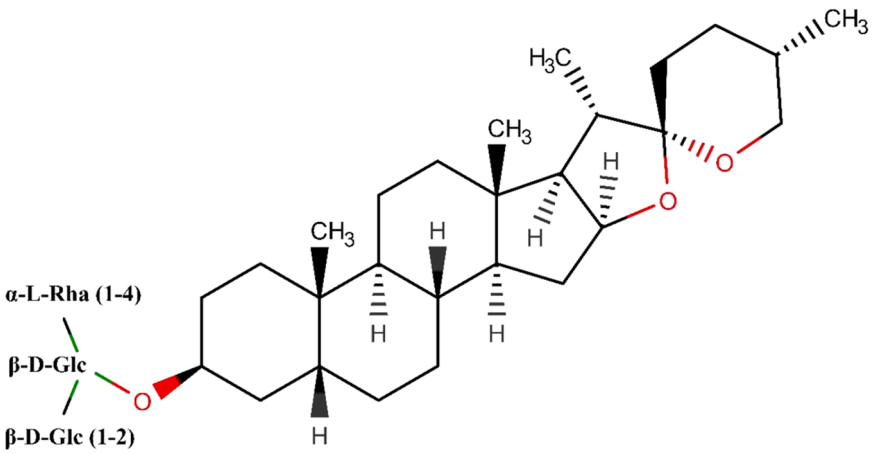

Fig. 1. Structure of Shatavarin IV.

used in a spectrophotometer (Thermo scientific evolution 201) at 660 nm to assess the available phosphorus. For the phosphorus quantification, the Bray 2 extractant method was used. (Bray and Kurtz, 1945). A conical flask was filled with 5 g of soil and 25 ml of 1 M ammonium acetate. After shaking for 5 mins, the solution was filtered. A photoelectric flame photometer was used to evaluate the filtrate for potassium estimate (Systronics model no: 126). Barium sulphate turbidimetric measurement was used to evaluate the amount of sulphur in soil samples (Page et al., 1982). A mixture of 0.500 g soil and 1.400 g sodium peroxide was prepared and the quantity of sulphate was evaluated using a turbidimeter (Digital Nephelo/Turbidity Meter, Systronics, Type 132). Organic carbon was oxidised with potassium dichromate to quantify total organic carbon in soil samples (1.5 N). The reaction took occurred in a sulphuric acid-rich atmosphere. After that, the oxidation product was analysed using a spectrophotometer for wet digestion (Nelson and Sommers, 1983).

The climatic conditions such as temperature average, temperature minimum, temperature maximum, annual rainfall, annual relative humidity, and ultraviolet radiation were taken as a monthly average of January, 2018-January, 2019 from Indian Metrological stations close to sample site (Table 3).

2.4. Artificial Neural Networks model development

The feed forward back propagation (BP) method was used to run the ANN model in Statistica 7 (Stat Soft Inc.). Two statistical algorithms namely, MLP (multilayer perceptron) and RBF (radial basis function) were used in ANN Model development for comparative study of prediction and optimization of Shatavarin IV. The ANN models of both the algorithms share some similar feature i.e., input layer (independent variables), hidden layer and output layer (dependent variable). The middle layer is called hidden layer which is the processing unit of the model. This layer is connected to both input and output layer. Each layer consists of neurons or nodes (Oludolapo et al., 2012). The MLP algorithm may have one or more hidden layers but there is only one hidden layer in RBF algorithm (Harpham et al., 2004). As we are comparing both model algorithms in the study, the number of hidden layers in MLP algorithm was set to one. The raw data is initially processed by input layer and then transferred to hidden layer where it is processed by different nonlinear activation or transfer function. No computational work is carried out in the input layer and all the weight calculations is being done by hidden layer. The hidden layer is the main processing unit of the model. In MLP, the activation or transfer function might be exponential, sine, logistic, tanh etc. The RBF model has only one activation function i.e., Gaussian basis function. After processing the data, the result is given through output layer. The difference between the expected and experimental data set would determine the model efficiency. The model algorithm recognises only the binary numbers. Therefore, all the variables were converted into 0 – 1 forms with the help of following formulae. This process is called normalisation of datasets.

$$X_{norm} = \frac{X - X_{min}}{X_{max} - X_{min}}$$

X_{norm}= normalised value of the variable.
X = Variable.
X_{max}=highest valued variable.
X_{min}=lowest valued variable.

The soil and climate factors were used as inputs, and Shatavarin IV was used as an output. Altitude, relative humidity, UV index, average temperature, minimum temperature, maximum temperature, annual precipitation, pH, organic carbon, electrical conductivity, nitrogen, phosphorus, potassium, and sulphur are used as the independent variables. In the current ANN model development, the amount of Shatavarin IV serves as the output dependent variable. A total of 103 germplasms were analysed in the model. The input variables of the samples were randomly partitioned into three subsets comprising of 70% data (73 accessions) for training, 15% data (15 accessions) for testing, and remaining 15% data (15 accessions) for ANN model validation. The network of each algorithm was trained for 10,000 iterations and the best model of each algorithm was selected. The number of neurons in the hidden layers were set in the range of 2–13 to create multiple feasible models. The activation function in the hidden layer governs various weights and biases in order to minimize the error between experimental and predicted value. The hidden and input layer neurons maintain and alter the dataset to produce the best results. The accurate models were selected based upon the training, testing and validation in terms of correlation coefficients. The correlation coefficient (R^2), root mean square error (RMSE), mean absolute error (MAE), and mean absolute percentage error (MAPE) were considered to determine the model predictive performance. The following formula were used.

$$R^2 = 1 - \frac{\sum_{i=1}^{n}(X_i - X_{ik})^2}{\sum_{n=i}^{n}(X_{ik} - X_z)^2}$$

$$RMSE = \frac{1}{n}\sum_{i=1}^{n}(X_i - X_{ik})^2$$

$$MAE = \frac{1}{n}\sum_{i=1}^{n}|X_i - X_{ik}|$$

Table 2
Physicochemical properties of soil samples collected from different geographical locations of Odisha.

Code	pH	EC (dS/m)	OC (%)	N (kg/ha)	P (kg/ha)	K (kg/ha)	S (ppm)
AR-1	5.130	0.180	0.190	0.370	6.250	144	38.011
AR-2	5.200	0.520	0.320	0.370	7.750	107	23.262
AR-3	5.130	0.180	0.190	150	42	144	38.011
AR-4	4.250	0.340	0.950	125	30	164.501	52.501
AR-5	5.810	0.090	0.750	105	25	361.901	30.502
AR-6	5.700	0.020	0.510	103	21	418.602	24.501
AR-7	6.420	0.100	0.120	167	38	225.603	6.252
AR-8	6.210	0.120	0.210	78	31	110.320	10
AR-9	5.860	0.170	0.290	56	12.320	89.262	16.252
AR-10	5.030	0.260	0.340	20	14.560	166.323	5
AR-11	6.210	0.120	0.210	6.720	6.720	110.321	10
AR-12	5.850	0.070	0.580	7.860	43.240	245.901	11.253
AR-13	5.850	0.070	0.580	7.860	43.240	245.901	11.253
AR-14	5.850	0.070	0.580	198	43.240	245.901	32.501
AR-15	5.850	0.070	0.580	145	43.240	245.901	32.501
AR-16	5.050	0.010	2.720	150	45.60	827.902	41.252
AR-17	5.100	0.010	2.910	187.500	40.50	713.603	41.252
AR-18	4.600	0.010	0.830	21	17	770.121	41.252
AR-19	4.540	0.310	1.880	11	26.401	528.191	12.981
AR-20	4.950	0.310	1.510	17	25.301	585.982	12.981
AR-21	4.860	0.310	0.700	125	18.602	733.821	12.981
AR-22	4.780	0.270	1.190	287.500	13.501	301.051	15.013
AR-23	4.810	0.270	0.740	37	17.402	299.713	15.013
AR-24	4.800	0.270	0.030	237	41.703	505.342	15.013
AR-25	4.53	0.270	0.740	200	45	480	15.013
AR-26	4.440	0.410	0.890	12.500	11.800	361.533	15.013
AR-27	3.050	0.410	0.540	161	31.501	783.551	13.701
AR-28	3.060	0.350	0.700	200	9.504	770.112	13.701
AR-29	3.030	0.350	0.650	199	10.012	780	16.102
AR-30	4.430	0.350	1.770	137.500	10.102	655.871	16.102
AR-31	4.350	0.350	0.930	187.500	12.301	215.041	16.102
AR-32	5.270	0.100	0.400	0.500	15	201	27.503
AR-33	5.270	0.100	0.400	0.500	15	201	27.503
AR-34	5.270	0.100	0.400	0.500	15	201	27.503
AR-35	5.420	0.390	1.010	22.900	16	700	15.441
AR-36	5.420	0.390	1.010	29.900	16	700	15.441
AR-37	7.550	0.340	0.910	8.700	19	675	19.671
AR-38	7.550	0.340	0.910	18.600	11	670	19.671
AR-39	7.550	0.340	0.910	188.600	9	677	19.671
AR-40	4.350	0.450	0.280	162.500	10	73.902	155
AR-41	4.351	0.410	0.280	162.500	23.300	73.900	187
AR-42	4.422	0.460	0.290	237.500	16.600	173.400	158
AR-43	4.422	0.490	0.290	37.500	16.600	173.400	167
AR-44	4.771	0.460	1.660	20	138.600	595.400	201
AR-45	4.771	0.500	1.660	22	138.600	595.400	198
AR-46	4.771	0.510	1.660	21	138.600	595.400	179
AR-47	4.390	0.150	1.450	162.500	18.300	248.600	21.200
AR-48	4.390	0.150	1.450	13.500	18.300	248.600	22.300
AR-49	4.390	0.150	1.450	15	18.300	248.600	21.500
AR-50	4.321	0.150	0.430	5	50.150	155.900	23
AR-51	3.811	0.150	1.150	10	32.200	247.300	20.900
AR-52	4.601	0.130	1.810	2.500	9.800	190.800	24.500
AR-53	3.910	0.200	1.880	30	16.500	177.400	26
AR-54	4.401	0.090	0.630	237.500	36.200	211.080	21.800
AR-55	4.202	0.120	0.820	50	23.900	514.700	22.600
AR-56	4.130	0.150	0.540	75	8.200	297.020	27.100
AR-57	3.810	0.200	0.740	262.500	35	178.750	23.900
AR-58	3.740	0.110	1.120	65	1.160	137.080	25.100
AR-59	3.690	0.160	0.990	350	39.700	229.820	21.300
AR-60	3.700	0.120	0.900	335	16	301.700	22.100
AR-61	3.620	0.100	1.010	340	21	290.450	25.700
AR-62	3.750	0.130	1	351	9	289.100	24.700
AR-63	3.820	0.450	0.480	262.500	18	327.930	23.500
AR-64	4.360	0.450	0.390	375	20	263.420	23.500
AR-65	3.790	0.450	0.430	162.500	27.600	568.610	23.500
AR-66	4.980	0.510	0.850	137.5	22.700	270.190	25.890
AR-67	4.850	0.510	1.530	187.500	37.300	423.360	25.890
AR-68	4.660	0.510	1.970	225	24.100	276.360	25.890
AR-69	4.640	0.430	1.400	275	30.800	615.550	30.450
AR-70	5.100	0.430	1.600	87.500	16.600	337.340	30.450
AR-71	4.870	0.430	1.300	21.500	8.700	485.800	30.450
AR-72	4.830	0.390	2.300	100.500	20	353.470	26.550
AR-73	4.300	0.390	2.550	162.500	19.800	370.940	26.550
AR-74	3.920	0.390	1.340	150	11.900	262.080	26.550

(*continued on next page*)

Table 2 (*continued*)

Code	pH	EC (dS/m)	OC (%)	N (kg/ha)	P (kg/ha)	K (kg/ha)	S (ppm)
AR-75	3.760	0.500	1.770	175	33.300	417.980	35.460
AR-76	3.780	0.500	2.100	125	32.500	440.830	35.460
AR-77	4.110	0.500	1.860	162.500	33.300	434.110	35.460
AR-78	3.860	0.470	1.420	137.500	20.600	491.900	33.270
AR-79	4.820	0.470	1.480	29	11.500	348.090	33.270
AR-80	5.380	0.470	1.260	25	15.700	565.800	33.270
AR-81	5.150	0.470	1.810	23	16.300	514.700	33.270
AR-82	5.160	0.310	2.380	31	14	424.700	30.100
AR-83	5.280	0.330	1.390	45	22.500	419.300	28.300
AR-84	5.080	0.450	2.140	237.500	20.200	352.500	32.010
AR-85	5.060	0.350	1.820	325	29.900	666.600	40.200
AR-86	4.890	0.290	3.090	137.500	21.200	276.800	34.800
AR-87	5.360	0.510	1.900	162.500	15.700	447.500	37.650
AR-88	5.200	0.470	1.660	29	10.700	315.800	40.500
AR-89	4.320	0.340	2.660	73	11.200	90.040	38.450
AR-90	4.780	0.390	2.850	67	20.200	333.300	31.050
AR-91	5.040	0.780	1.560	112.500	26.900	518.700	45.100
AR-92	4.780	0.650	2.080	11.500	18	467.700	50.320
AR-93	5.200	0.910	1.730	21.500	15.300	245.900	46.890
AR-94	5.220	0.890	2.850	17.500	15.500	334.560	51.670
AR-95	5.150	0.530	3.690	25	16.900	733.810	50.540
AR-96	3.190	0.450	0.410	200	36.300	383.040	25.100
AR-97	4.700	1.030	3.800	100	25.300	447.550	23.200
AR-98	4.930	0.990	1.560	200	37.100	756.670	25.440
AR-99	4.420	0.890	1.470	225	37	633.020	30.000
AR-100	4.170	0.910	1.640	285	39.100	297.020	27.560
AR-101	5.220	1.450	3.520	150	18	848.060	356.100
AR-102	5.220	2.030	3.520	150	18	848.060	324.400
AR-103	5.220	1.990	3.520	150	18	848.060	338.900

AR-Asparagus racemosus, EC- electrical conductivity, OC – organic carbon, N-nitrogen, P-phosphorus, K-potassium, S-sulphur, dS/m-deciSiemens per meter, kg-Kilogram, ha- hectare, ppm- parts per million

$$\text{MAPE} = \frac{1}{n}\sum_{i=1}^{n}|X_i - X_{ik}| \times 100$$

Here,
x_i =predicted value,
x_{ik} = experimental value,
x_z =mean of experimental value and.
n = number of observations.

3. Results and discussion

3.1. Variation in the Shatavarin IV

The samples were analyzed in HPTLC and the variations were determined in Shatavarin IV content. The detection of the Shatavarin IV was initially done on the basis of retardation factor (R_f) of both standard and samples. It was detected at R_f of 0.400 ± 0.050. The detection compound was confirmed by comparing the absorption spectra of both standard Shatavarin IV and *Asparagus racemosus* samples (Fig. 2) where absorption maxima were at 425 nm. The 2D densitogram of Shatavarin IV (Fig. 3) shows the R_f of 0.400 ± 0.050. The standard curve of Shatavarin IV showed a good linear relationship within a concentration range of 72–432 ng/band (Fig. 4). The regression analysis showed a coefficient of determination (R^2) of 0.997. The Shatavarin IV was quantified in samples by using the regression equation i. e., y = 779.455 + 14.254x (y-area unit and x-amount of Shatavarin IV) of the calibration curve and expressed in percentage (%). The standard deviation of the calibration curve was found to be 3.890%. The limit of detection (LOD) is the minimum concentration of an analyte at which the peak area of the signal is at least three times greater than signal to noise ratio (S/N ≥ 3) which was found to be 24 ng/spot. The limit of quantification (LOQ) is the lowest concentration of an analyte at which the signal is at least ten times greater than the noise (S/N ≥ 10) and it was found to be 72 ng/spot. The method of quantitative analysis showed satisfactory results in precision, stability and recovery tests. The relative standard deviation (RSD) of precision and stability was found to be 1.630% and 1.690% respectively and were in the acceptable range. The recovery percentage of Shatavarin IV was found to be more than 97% with RSD value of 0.970%. The representative HPLTC chromatogram of *A. racemosus* was given in the Fig. 5.

The amount of Shatavarin IV varied significantly from different regions of Odisha. The range was in between 0.010% and 0.400% among the samples. To eliminate seasonal and developmental fluctuation in secondary metabolites, the *A. racemosus* samples were taken during a single growing season with identical growth phase. Plant ontogeny, environmental, and genetic factors contribute to intraspecific chemical diversity (Moore et al., 2014). Plant secondary metabolites have also been shown to vary geographically (Chen et al., 2015). Seasonal and developmental differences might not have played an impact in our study since the samples were taken from a single growing season at similar growth stages. The fluctuation in Shatavarin IV in the current study might be ascribed to soil conditions, climate change, and gene expression levels which need to be investigated further. The possible cause of variation in Shatavarin IV due to soil conditions and climatic change is investigated in this research work by using a statistical prediction model. The variation of shatavarin IV among various population of *A. racemosus* was reported by some researchers (Saran et al., 2020). The variability of Shatavarin IV was also reported from the other species of *Asparagus* (Saran et al., 2021). The variability or low Shatavarin IV contents in the raw plant material leads to low quality material which results in the drug adulteration in herbal medicines and herbal products. Also, the inconsistency in the biologically active compounds in plant material may affect the efficacy and safety of the drug (Van Wyk and Prinsloo, 2020).

3.2. ANN model analysis

The neural network model is a useful tool for classifying and predicting experimental data sets. (Akbar et al., 2016). By critically analysing the soil and climatic conditions, the current study exploited the ability of artificial neural network (ANN) to forecast the Shatavarin IV content in *A. racemosus*. The best models of MLP and RBF algorithm is

Table 3
Climatic data for 103 *Asparagus racemosus* accessions from different geographical regions of Odisha.

Code	Altitude	Annual Precipitation	Max temp.	Min temp.	Average temp.	Annual RH	UV Index
AR-1	131	1396	38.200	14.700	27.200	65.400	6.700
AR-2	64	1516	37.300	14.500	26.900	65.400	6.700
AR-3	131	1396	38.200	14.700	27.200	65.400	6.700
AR-4	18	1428	36.100	15.700	27.200	67.500	6.700
AR-5	19	1428	36.100	15.700	27.200	67.500	6.700
AR-6	20	1428	36.100	15.700	27.200	67.500	6.700
AR-7	448	1312	36.700	14.900	26.500	68.600	6.600
AR-8	388	1312	36.700	14.900	26.500	68.600	6.600
AR-9	249	1312	36.700	14.900	26.500	68.600	6.600
AR-10	415	1312	36.700	14.900	26.500	68.600	6.600
AR-11	360	1312	36.700	14.900	26.500	68.600	6.600
AR-12	658	1245	33.400	13.700	24.800	67.000	6.800
AR-13	658	1248	33.400	13.700	24.800	67.000	6.800
AR-14	658	1247	33.400	13.700	24.700	67.000	6.800
AR-15	827	1245	33.400	13.700	24.800	67.000	6.800
AR-16	1089	1670	38	17	28.300	66.350	6.810
AR-17	1089	1670	38	17	28.300	66.350	6.810
AR-18	1089	1670	38	17	28.300	60.350	6.810
AR-19	723	1670	38	17	28.300	60.350	6.670
AR-20	723	1670	38	17	28.300	60.350	6.670
AR-21	572	1670	38	17	28.300	60.350	6.670
AR-22	741	1245	33.400	13.700	24.800	67	6.750
AR-23	741	1245	33.400	13.700	24.800	67	6.750
AR-24	741	1245	33.400	13.700	24.800	67	6.750
AR-25	741	1245	33.400	13.700	24.800	67	6.750
AR-26	76	1245	33.400	13.700	24.800	67	6.750
AR-27	94	1245	33.400	13.700	24.800	67	6.750
AR-28	100	1245	33.400	13.700	24.800	67	6.750
AR-29	476	1245	33.400	13.700	24.800	67	6.750
AR-30	476	1245	33.400	13.700	24.800	67	6.750
AR-31	476	1245	33.400	13.700	24.800	67	6.750
AR-32	116	1472	37.900	14.600	27	65.900	6.800
AR-33	116	1472	37.900	14.600	27	65.900	6.800
AR-34	117	1472	37.900	14.600	27	65.900	6.800
AR-35	257	1249	40	13.400	26.900	57.900	6.800
AR-36	258	1249	40	13.400	26.900	57.900	6.800
AR-37	182	1249	40	13.400	26.900	57.900	6.800
AR-38	182	1249	40	13.400	26.900	57.900	6.800
AR-39	182	1249	40	13.400	26.900	57.900	6.800
AR-40	8	1337	32.500	17.100	26.900	73.750	7.250
AR-41	8	1337	32.500	17.100	26.900	73.750	7.250
AR-42	8	1337	32.500	17.100	26.900	73.750	7.250
AR-43	8	1337	32.500	17.100	26.900	73.750	7.250
AR-44	8	1337	32.500	17.100	26.900	73.750	7.250
AR-45	8	1337	32.500	17.100	26.900	73.750	7.250
AR-46	8	1337	32.500	17.100	26.900	73.750	7.250
AR-47	634	1667	35.500	11.300	23.600	62.910	6.410
AR-48	634	1667	35.500	11.300	23.600	62.910	6.410
AR-49	634	1667	35.500	11.300	23.600	62.910	6.410
AR-50	634	1667	35.500	11.300	23.600	62.910	6.410
AR-51	634	1667	35.500	11.300	23.600	62.910	6.410
AR-52	634	1667	35.500	11.300	23.600	62.910	6.410
AR-53	511	1667	35.500	11.300	23.600	62.910	6.410
AR-54	634	1667	35.500	11.300	23.600	62.910	6.410
AR-55	634	1667	35.500	11.300	23.600	62.910	6.410
AR-56	634	1667	35.500	11.300	23.600	62.910	6.410
AR-57	634	1667	35.500	11.300	23.600	62.910	6.410
AR-58	688	1667	35.500	11.300	23.600	62.910	6.410
AR-59	688	1667	35.500	11.300	23.600	62.910	6.410
AR-60	94	1667	35.500	11.300	23.600	62.910	6.410
AR-61	86	1667	35.500	11.300	23.600	62.910	6.410
AR-62	94	1667	35.500	11.300	23.600	62.910	6.410
AR-63	128	1686	37.500	15.200	26.800	68.350	6.750
AR-64	128	1686	37.500	15.200	26.800	68.350	6.750
AR-65	128	1686	37.500	15.200	26.800	68.350	6.750
AR-66	244	1686	37.500	15.200	26.800	68.350	6.750
AR-67	244	1686	37.500	15.200	26.800	68.350	6.750
AR-68	244	1686	37.500	15.200	26.800	68.350	6.750
AR-69	244	1686	37.500	15.200	26.800	68.350	6.750
AR-70	244	1686	37.500	15.200	26.800	68.350	6.750
AR-71	244	1686	37.500	15.200	26.800	68.350	6.750
AR-72	81	1686	37.500	15.200	26.800	68.350	6.750
AR-73	81	1686	37.500	15.200	26.800	68.350	6.750

(*continued on next page*)

Table 3 (*continued*)

Code	Altitude	Annual Precipitation	Max temp.	Min temp.	Average temp.	Annual RH	UV Index
AR-74	81	1686	37.500	15.200	26.800	68.350	6.750
AR-75	81	1686	37.500	15.200	26.800	68.350	6.750
AR-76	81	1686	37.500	15.200	26.800	68.350	6.750
AR-77	81	1686	37.500	15.200	26.800	68.350	6.750
AR-78	124	1686	37.500	15.200	26.800	68.350	6.750
AR-79	124	1686	37.500	15.200	26.800	68.350	6.750
AR-80	124	1686	37.500	15.200	26.800	68.350	6.750
AR-81	124	1686	37.500	15.200	26.800	68.350	6.750
AR-82	296	978	40.800	9.500	25.800	62.250	6.520
AR-83	296	978	40.800	9.500	25.800	62.250	6.520
AR-84	296	978	40.800	9.500	25.800	62.250	6.520
AR-85	296	978	40.800	9.500	25.800	62.250	6.520
AR-86	296	978	40.800	9.500	25.800	62.250	6.520
AR-87	296	978	40.800	9.500	25.800	62.250	6.520
AR-88	296	978	40.800	9.500	25.800	62.250	6.520
AR-89	296	978	40.800	9.500	25.800	62.250	6.520
AR-90	296	978	40.800	9.500	25.800	62.250	6.520
AR-91	188	1499	43	14	27	54	6.760
AR-92	181	1499	43	14	27	54	6.760
AR-93	181	1499	43	14	27	54	6.760
AR-94	181	1499	43	14	27	54	6.760
AR-95	181	1499	43	14	27	54	6.760
AR-96	340	1403	37.500	12	25.700	42	6.700
AR-97	798	1403	37.500	12	25.700	42	6.700
AR-98	693	1403	37.500	12	25.700	42	6.700
AR-99	693	1403	37.500	12	25.700	42	6.700
AR-100	763	1403	37.500	12	25.700	42	6.700
AR-101	43	1410	33.800	17.700	26.800	67.300	6.500
AR-102	44	1410	33.800	17.700	26.800	67.300	6.500
AR-103	45	1410	33.800	17.700	26.800	67.300	6.500

AR-Asparagus racemosus, Temp. – Temperature, RH- Relative humidity, UV- Ultra violet, Max-maximum, Min-minimum.

given in the Table 4. Our study found that, the MLP algorithm has a better predictive performance as compared to RBF algorithm. The best model of the MLP algorithm was found to have 14–8–1 architecture (Fig. 6). The RBF algorithm has simple network structure, faster learning processes and better estimation capability. This characteristic makes the RBF model as one of the popularly used algorithm in scientific and engineering applications (Benghanem and Mellit, 2010; Mellit and Kalogirou, 2008). There are different types of radial basis functions which act

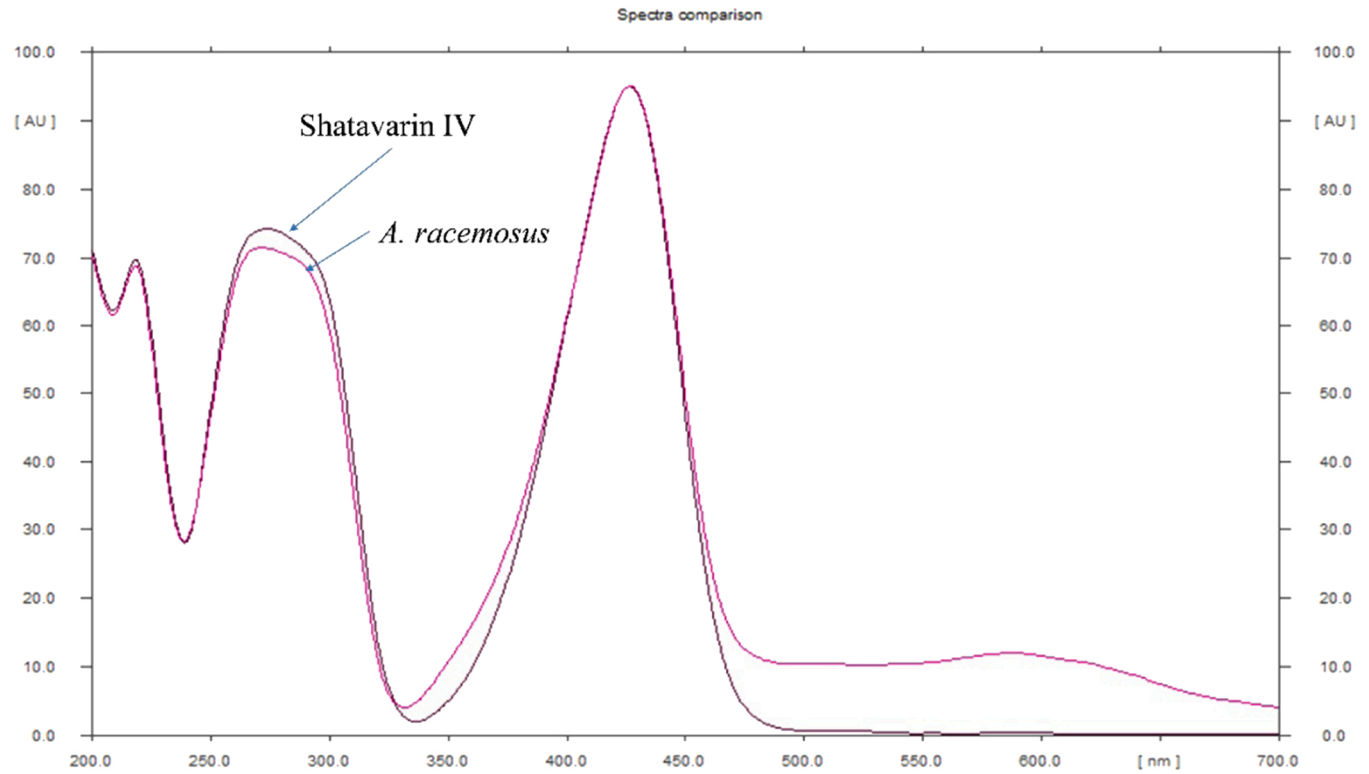

Fig. 2. Absorption spectra of Shatavarin IV and *Asparagus racemosus*.

as activation or transfer functions in hidden layer (Ghorbani et al., 2016). The most widely used activation function of RBF algorithm have been used in our study, is the Gaussian activation function. The output layer gave the results in the form of Identity activation function. Although, different algorithms of artificial neural network models have been developed, MLP-ANN model is still most widely used model (Mata, 2011). As both the algorithms have their application advantage in various fields, they have been used in the current study.

The model selected as best in our study was MLP-ANN which showed the coefficient of determination (R^2) between predicted and observed values of the Shatavarin IV in training, testing and validation datasets as 0.985, 0.989 and 0.992 respectively (Fig. 7). The RMSE of observed and predicted values are 0.012, 0.012 and 0.010 for training, testing and validation respectively. The observed and predicted content of Shatavarin IV through training, testing and validation were given in the Tables 5–7 respectively. The outputs of coefficient of determination (R^2) and RMSE of the developed ANN model were within the admissible ideal range. The value of coefficient of determination (R^2) close to 1 and value of RMSE close to 0 are regarded as ideal in statistical analysis. Among different activation functions used for hidden layer processing in our study, the exponential activation function was found to gave the best model output. The output result in ANN-MLP was given by identity activation function.

The multi-layer perceptron (MLP) of feed-forward type is the most prevalent and popular ANN model. This model mimics the functioning of a human brain with numerous neurons (Sheikh and Unde, 2012). The MLP has a wide range of applications in a variety of domains, including pattern recognition, prediction, classification, and function approximation (Golovko et al., 2000). The MLP-ANN model has a number of advantages than conventional statistical methods. This model efficiently introduces nonlinearity to the data analysis process. The data analysis in this model is dynamic in nature i.e., it can learn to adjust to the new conditions (Le et al., 2020). Based on its statistical criteria, MLP-ANN was regarded as best algorithm than RBF-ANN model algorithm in a prediction and optimization study (Amedi et al., 2016). In another study, MLP with Broyden–Fletcher–Goldfarb–Shanno (BFGS) learning algorithm was found to be more efficient than RBF with radial basis function network for prediction of landslide susceptibility mapping (Zare et al., 2013).

The ANN model of MLP algorithm has been used by various researchers for prediction and optimization of secondary metabolites in medicinal plants. MLP algorithm in ANN model have been the primary choice of the researchers in the field of secondary metabolites prediction and optimization in plants. The content of andrographolide in *Andrographis paniculata* was predicted and optimized through ANN model of MLP algorithm (Champati et al., 2022). Similarly, the content of bacoside A content in *Bacopa monnieri* was optimized and predicted through MLP algorithm of ANN model (Padhiari et al., 2022). The ANN-MLP model was used to predict the content of coronarin D in *H. coronarium* (Ray et al., 2020). Similarly, the content of podophyllotoxin, the bioactive constituent of *Podophyllum hexandrum*, was assessed through the ANN-MLP model (Alam and Naik, 2009). In addition, the ANN-MLP model was used to forecast and optimize the essential oil and curcumin content in turmeric (Akbar, and Akbar et al., 2016, 2018).

3.3. Sensitivity analysis

Sensitivity analysis is critical for determining the most essential factors that influence the amount of Shatavarin IV in *A. racemosus*. This study allows us to determine the rate at which the model output changes as input parameters in the model change, as well as to identify the input parameters that have the most impact on the model's output (Jimeno-Sáez et al., 2018). The sensitive analysis of the ANN model prediction study on the content of Shatavarin IV in *A. racemosus* revealed that

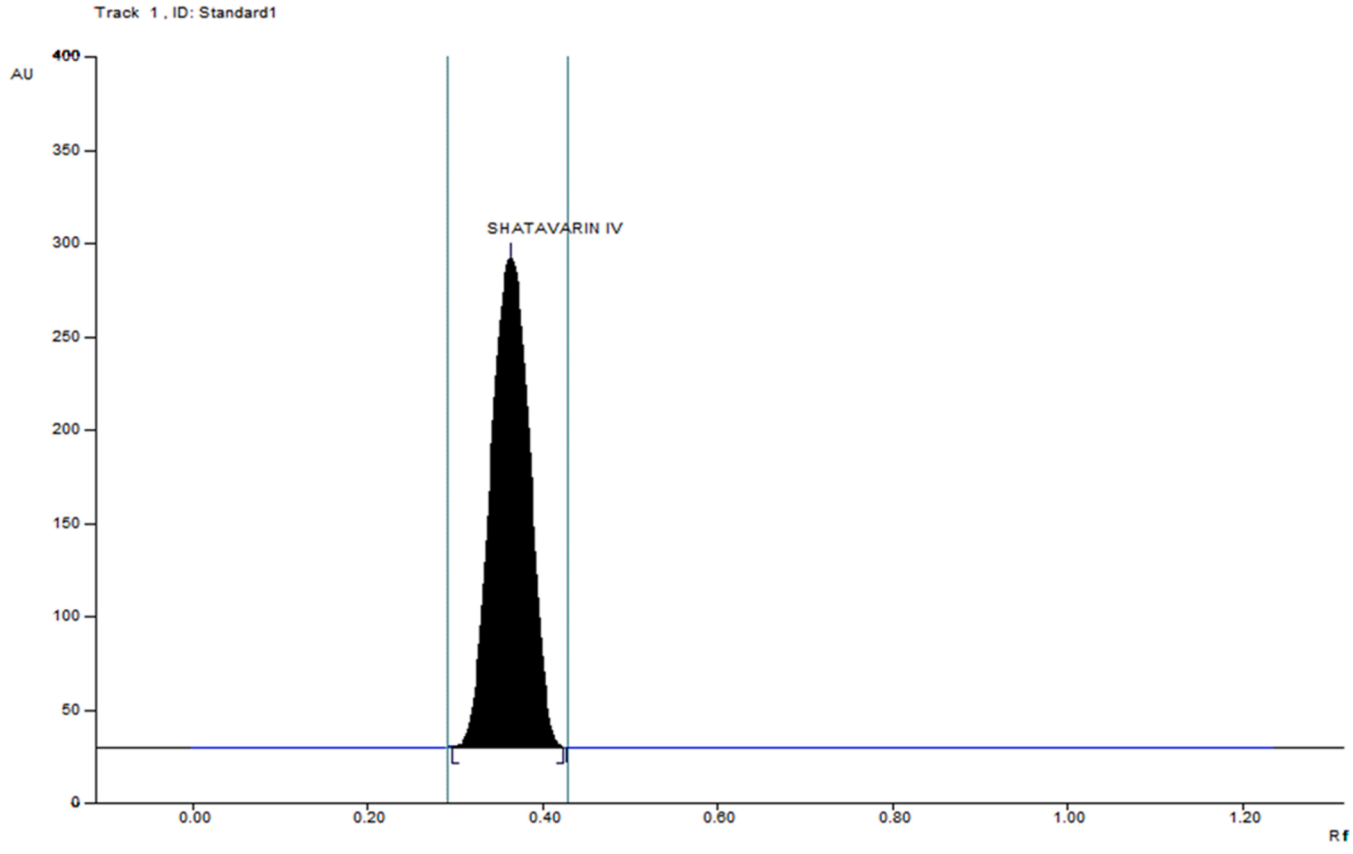

Fig. 3. 2D HPTLC densitogram of Shatavarin IV.

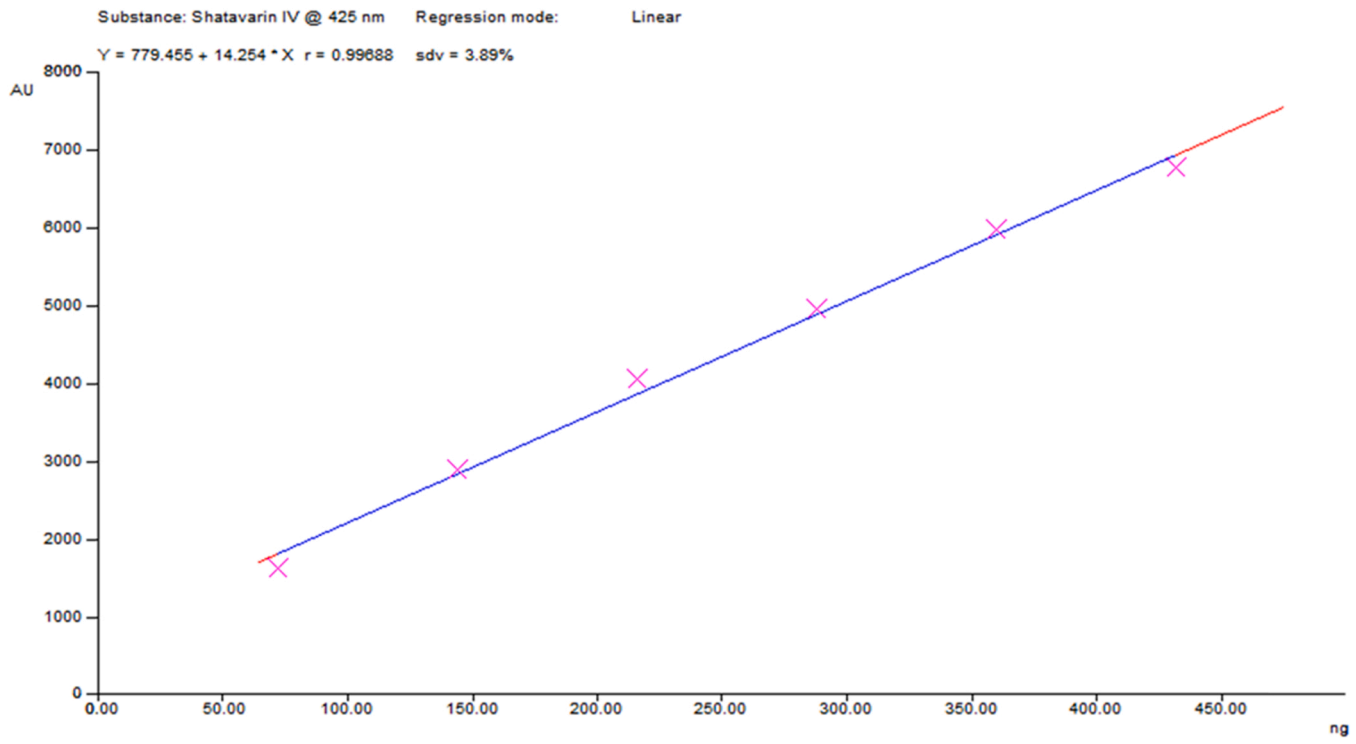

Fig. 4. Calibration curve of Shatavarin IV for quantitative analysis.

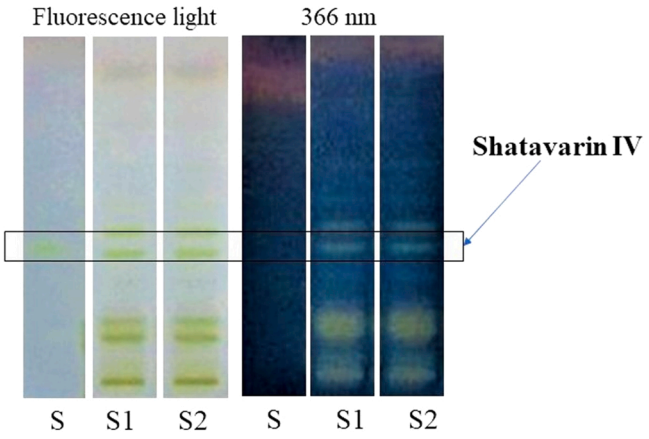

Fig. 5. HPTLC fingerprint of Shatavarin IV and *Asparagus racemosus* (S-standard, S1– sample 1 and S2– sample 2).

nitrogen (N) and phosphorus (P) content in the soil greatly affect the Shatavarin IV content. The N an P has the highest sensitivity error quotient of 3.586 and 2.796 respectively. Average temperature preceded the list of sensitive factors next to N and P with an error quotient of 1.6441. The error quotient of all the factors studied in this investigation have been given in the Table 8.

There are a number of external internal factors which are responsible for growth and development in plants. Among various important factors, nutrients play a vital role in growth and development in plants. Macro-nutrients and micro-nutrients are required in different optimal concentration for the proper functioning of normal physiological balance in plants. The appropriate growth, yield and herbal quality in plants largely depend on the amount of macro-nutrients (Tripathi et al., 2014). In plants, an optimum level of all nutrients is required for carrying out the cellular processes necessary for their growth and development. In general, the elements like nitrogen (N), phosphorus (P), and potassium (K) are those that plants require the most and play a significant role in ensuring proper growth and development (Muller et al., 2013). Our study revealed that higher level of nitrogen accompanied a higher content of Shatavarin IV in *A. racemosus*. The saponin biosynthesis has a direct relationship with appropriate nitrogen level in the soil. The increase in the nitrogen uptake resulted in the accumulation of saponins in *Panax notoginseng*. The study suggested that, nitrogen promotes the saponins synthesis and regulate the nutrient uptake (Wei et al., 2020) but the limit of increase in N_2 level upto which the saponin accumulation increases is still under research. The mechanistic study on the nitrogen driven regulation of saponins suggested that the activity of β-glucosidase is reduced and thereby increasing the saponins accumulation in low nitrogen level. Further, the study says that the ability of roots to absorb nitrogen was a crucial determinant in determining the direction and degree of improvement in saponin content (Zhang et al., 2020). The saponin accumulation increases with an increase in nitrogen upto 382.7 mg/l and then sharply declines in *Panax ginseng* (Kim et al., 2005). Therefore, the upper and lower limit of nitrogen for optimum level of saponin biosynthesis need to be explored precisely. Phosphorus is the second sensitive factors after nitrogen which affects the Shatavarin IV content in our study. It is one of the important macro-nutrients required relatively in large amount as it is involved in primary and secondary metabolites production in plants (Nell et al., 2009).

Table 4
Best model of MLP and RBF out of 10,000 iterations.

Net. name	Training perf.	Test perf.	Validation perf.	Training error	Test error	Validation error	Hidden activation	Output activation
MLP 14–8–1	**0.972**	**0.970**	**0.972**	**0.002**	**0.007**	**0.002**	**Exponential**	**Identity**
RBF 14–13–1	0.924	0.931	0.873	0.004	0.008	0.004	Gaussian	Identity

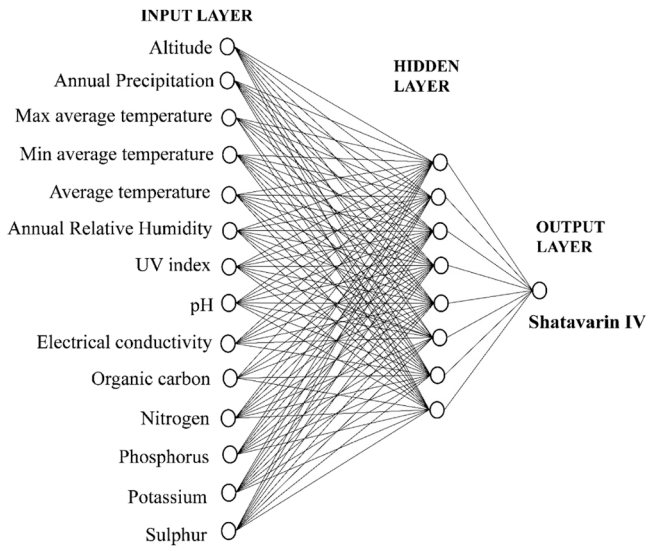

Fig. 6. Architecture of the multilayer perceptron feed-forward network used in the study.

Phosphorus plays a major role in the production and accumulation of saponins and sapogenin synthesis in plants (Muller et al., 2013). The effect of phosphate concertation on cell growth and saponin accumulation was studied previously. In a previous study, it was observed that the increasing phosphate concentration upto a certain upper limit resulted in increased saponin production but after that it was declined to certain extend in further increase of phosphate concentration in *Panax notoginseng* (Zhong and Zhu, 1995). The optimal concentration of phosphate for maximum saponin production in *Panax ginseng* and *Panax quinquefolium* was determined to be 643 mg/L (Liu et al., 1998). The optimization study in our investigation was also revealed that increasing phosphate concentration increases Shatavarin IV. However, the optimal concentration and role of phosphate in Shatavarin IV production in *A. racemosus* is to be explored further. Temperature preceded the nitrogen and phosphorus in the row of sensitive factors affecting the Shatavarin IV content. In root tissues of *Panax ginseng* C.A. Meyer, photosynthetically active radiation and soil water potential had a greater impact on ginsenoside (saponin) accumulation and in case of leaf tissues, temperature and humidity had a greater impact (Zhang et al., 2018). Previous studies had also indicated that *A. racemosus* can be cultivated as an intercrop in 25% shade-net intensities with higher Shatavarin content (Saran et al., 2019). Shed net intensity of 25% refers to the temperature of less than 28 °C roughly (Gaurav et al., 2014) which is close to average temperature for the samples collected in our study. The medicinal plants encounter smoother growth in a place with partial shade, moderate temperature, high relative intensity and moist soil rich in organic matters (Venugopal et al., 2008).

The sensitivity analysis revealed that soil parameters have a more significant effect than climatic factors on the biosynthesis of Shatavarin IV in *A. racemosus*. Moreover, soil nitrogen and phosphorus content seem to play a crucial role either directly or indirectly as activators in triggering biosynthetic pathway of Shatavarin IV. The exact role of nitrogen and phosphorus needs to be investigated further.

3.4. Application of the ANN model at a new site

The ANN model developed was used to predict the Shatavarin IV content yield in *A. racemosus* samples collected from new site at Budisila, Gajapati, Odisha (Fig. 8). The soil and climate variables were recorded earlier for use in this model. The model predicted Shatavarin IV content as 0.245% on dry weight basis. The predicted value obtained from the model by using soil and climatic factors was validated using HPTLC analysis by collecting samples of *A. racemosus*, from the same site that exhibited Shatavarin IV content to be 0.270% on dry weight basis. The ANN model showed an accuracy of 90.740% in predicting the

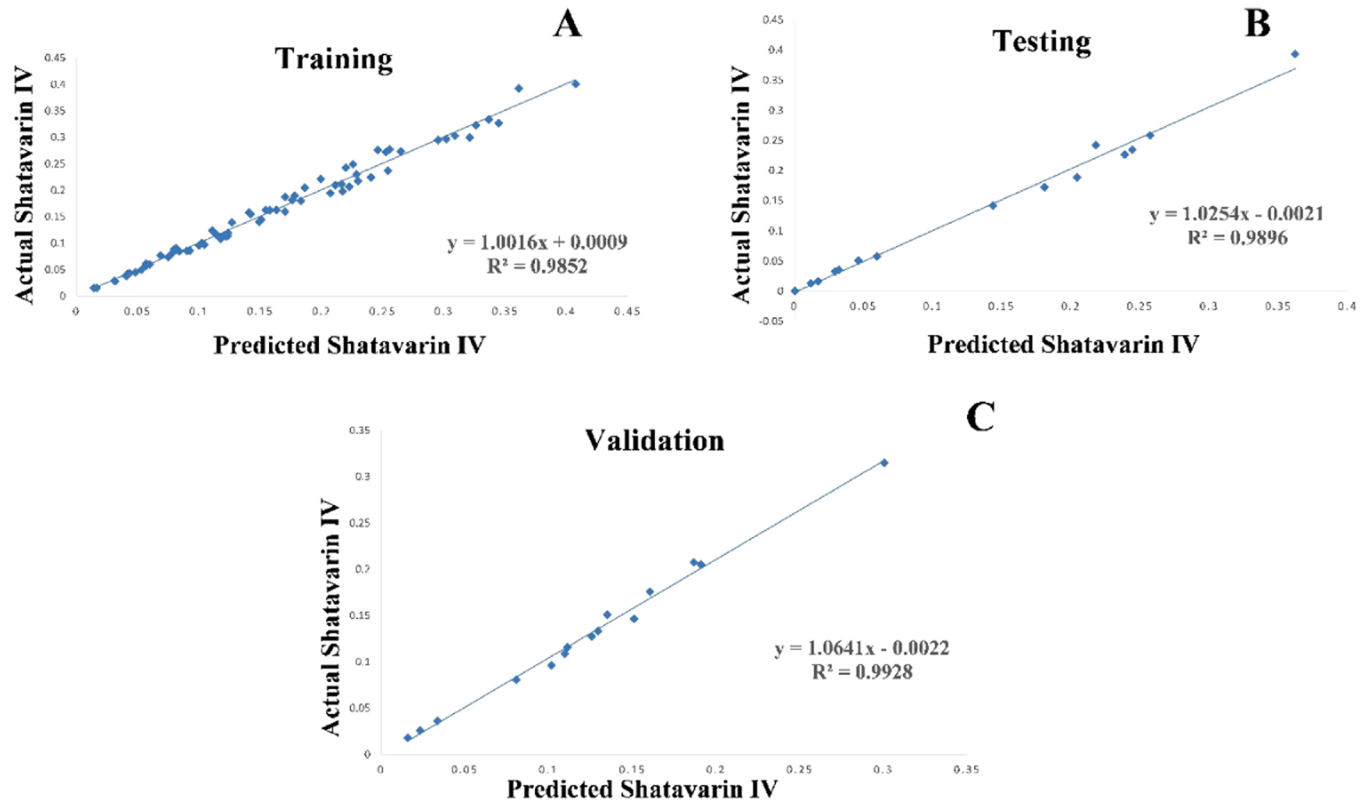

Fig. 7. Scatter showing experimental and predicted values of Shatavarin IV in training (A), testing (B), and validation (C).

Table 5
Actual and predicted Shatavarin IV content of training dataset.

Sample code	Predicted Shatavarin IV (%)	Observed Shatavarin IV (%)	AE	APE
AR-2	0.142	0.156	0.015	9.520
AR-3	0.345	0.327	0.018	5.468
AR-4	0.230	0.218	0.012	5.647
AR-5	0.211	0.210	0.001	0.561
AR-6	0.229	0.230	0.001	0.587
AR-7	0.336	0.334	0.003	0.777
AR-8	0.199	0.221	0.022	9.861
AR-10	0.163	0.163	0.000	0.081
AR-12	0.252	0.272	0.020	7.354
AR-14	0.361	0.392	0.031	8.004
AR-17	0.240	0.224	0.016	7.191
AR-18	0.092	0.086	0.007	7.583
AR-20	0.090	0.086	0.005	5.349
AR-22	0.154	0.163	0.008	5.006
AR-24	0.407	0.401	0.006	1.539
AR-26	0.127	0.139	0.012	8.800
AR-27	0.254	0.237	0.017	7.282
AR-28	0.226	0.250	0.024	9.599
AR-29	0.102	0.101	0.002	1.715
AR-30	0.104	0.097	0.007	7.128
AR-31	0.040	0.039	0.001	3.166
AR-33	0.042	0.041	0.000	0.924
AR-34	0.053	0.050	0.003	6.451
AR-35	0.123	0.114	0.010	8.706
AR-36	0.122	0.113	0.010	8.645
AR-40	0.031	0.029	0.002	7.156
AR-42	0.114	0.117	0.003	2.547
AR-43	0.084	0.085	0.001	0.789
AR-44	0.069	0.077	0.008	10.558
AR-46	0.124	0.120	0.004	3.382
AR-48	0.043	0.043	0.000	0.691
AR-49	0.016	0.015	0.001	6.484
AR-51	0.060	0.060	0.000	0.270
AR-52	0.032	0.029	0.003	8.995
AR-55	0.100	0.096	0.004	4.139
AR-56	0.048	0.045	0.003	7.523
AR-58	0.057	0.062	0.005	8.298
AR-59	0.302	0.297	0.005	1.658
AR-61	0.111	0.124	0.013	10.531
AR-62	0.014	0.015	0.001	7.436
AR-63	0.141	0.158	0.017	10.932
AR-64	0.081	0.091	0.010	10.607
AR-65	0.186	0.205	0.019	9.162
AR-67	0.265	0.273	0.009	3.251
AR-68	0.142	0.155	0.013	8.543
AR-69	0.176	0.181	0.005	2.834
AR-70	0.151	0.145	0.006	3.986
AR-73	0.217	0.198	0.019	9.761
AR-74	0.117	0.111	0.006	5.565
AR-75	0.220	0.243	0.023	9.449
AR-76	0.170	0.188	0.018	9.326
AR-77	0.321	0.299	0.021	7.171
AR-79	0.075	0.074	0.001	1.811
AR-80	0.041	0.041	0.000	0.001
AR-81	0.041	0.039	0.002	5.163
AR-83	0.080	0.089	0.009	9.953
AR-84	0.246	0.276	0.030	10.870
AR-85	0.326	0.323	0.003	0.903
AR-86	0.207	0.195	0.013	6.484
AR-88	0.078	0.081	0.003	3.642
AR-89	0.170	0.160	0.010	6.548
AR-90	0.149	0.141	0.008	5.994
AR-92	0.118	0.108	0.009	8.690
AR-93	0.122	0.115	0.006	5.333
AR-94	0.057	0.057	0.001	0.998
AR-95	0.158	0.162	0.004	2.641
AR-96	0.256	0.277	0.021	7.715
AR-97	0.216	0.211	0.005	2.408
AR-98	0.222	0.207	0.016	7.572
AR-99	0.295	0.295	0.000	0.003
AR-100	0.309	0.303	0.006	2.001
AR-102	0.178	0.190	0.012	6.314
AR-103	0.183	0.180	0.003	1.693
MAE	–	–	0.009	–
MAPE	–	–	–	5.544
RMSE	0.012	–	–	–

AR-Asparagus racemosus, AE- Absolute error, APE- Absolute percentage error, MAE-Mean absolute error, Mean absolute percentage error, RMSE-Root mean square error.

Table 6
Actual and predicted Shatavarin IV content of testing dataset.

Sample code	Predicted Shatavarin IV (%)	Observed Shatavarin IV (%)	AE	APE
AR-1	0.046	0.051	0.004	8.825
AR-9	0.204	0.189	0.016	8.333
AR-11	0.181	0.173	0.008	4.660
AR-13	0.218	0.243	0.025	10.189
AR-16	0.244	0.235	0.009	3.907
AR-21	0.032	0.036	0.003	9.515
AR-25	0.362	0.393	0.032	8.020
AR-38	0.001	0.001	0.000	0.370
AR-45	0.060	0.058	0.002	3.354
AR-57	0.257	0.259	0.002	0.587
AR-60	0.012	0.013	0.001	6.461
AR-66	0.144	0.142	0.001	0.950
AR-71	0.029	0.033	0.003	9.464
AR-82	0.017	0.016	0.001	3.487
AR-91	0.239	0.227	0.012	5.234
MAE	–	–	0.008	–
MAPE	–	–	–	5.557
RMSE	0.012	–	–	–

AR-Asparagus racemosus, AE- Absolute error, APE- Absolute percentage error, MAE-Mean absolute error, Mean absolute percentage error, RMSE-Root mean square error.

Table 7
Actual and predicted Shatavarin IV content of validation dataset.

Sample code	Predicted Shatavarin IV (%)	Observed Shatavarin IV (%)	AE	APE
AR-15	0.301	0.315	0.014	4.503
AR-19	0.081	0.081	0.000	0.173
AR-23	0.102	0.096	0.006	5.938
AR-32	0.187	0.207	0.021	9.924
AR-37	0.034	0.036	0.003	7.435
AR-39	0.016	0.018	0.002	10.858
AR-41	0.151	0.147	0.004	3.010
AR-47	0.110	0.109	0.001	0.702
AR-50	0.023	0.026	0.002	9.017
AR-53	0.111	0.116	0.005	3.990
AR-54	0.191	0.205	0.014	6.909
AR-72	0.135	0.151	0.016	10.658
AR-78	0.130	0.133	0.004	2.768
AR-87	0.126	0.127	0.001	1.174
AR-101	0.161	0.176	0.015	8.511
MAE	–	–	0.007	–
MAPE	–	–	–	5.705
RMSE	0.010	–	–	–

AR-Asparagus racemosus, AE- Absolute error, APE- Absolute percentage error, MAE-Mean absolute error, Mean absolute percentage error, RMSE-Root mean square error.

Shatavarin IV content at a new site. The present ANN model therefore was found to be significantly useful and reliable for future applications in analysing Shatavarin IV content in *A. racemosus* accession collected from anywhere without physically collecting/uprooting the plants from the wild. With proper climate and soil conditions determined, the developed ANN model would be a useful tool in identifying collection sites of elite accessions of *A. racemosus* with high Shatavarin IV content.

Table 8
Error quotients and their rank of sensitive parameters of the neural network.

Parameters	Error quotient	Rank
Nitrogen (kg/ha)	3.586	1
Phosphorus (kg/ha)	2.796	2
Average temperature	1.644	3
UV Index	1.587	4
Minimum temperature	1.509	5
Annual Precipitation	1.502	6
Max temperature	1.214	7
Sulphur (ppm)	1.220	8
Potassium (kg/ha)	1.084	9
Annual Relative Humidity	1.067	10
pH	1.058	11
Electrical Conductivity (dS/m)	1.042	12
Organic Carbon (%)	1.012	13
Altitude	0.998	14

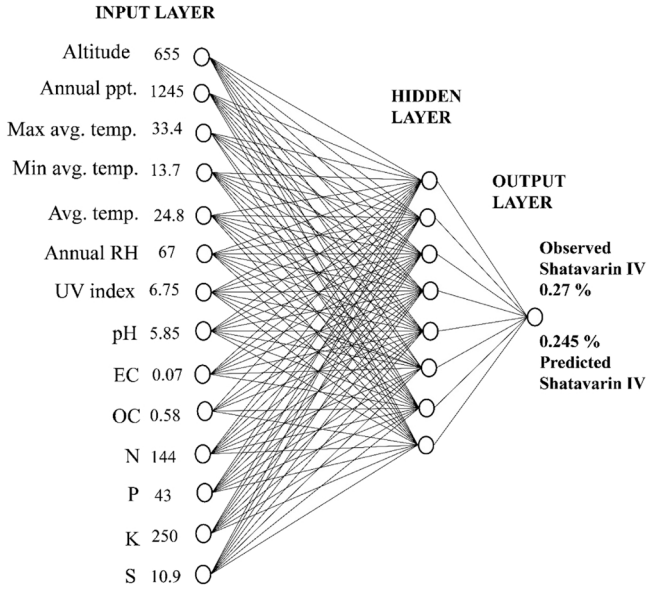

Fig. 8. Application of the ANN model at new site for prediction of Shatavarin IV content. (ppt.-precipitation, max.-maximum, min.-minimum, avg.-average, temp.-temperature, RH-relative humidity, EC-electrical conductivity, OC-organic carbon, N-nitrogen, P-phosphorus, K-potassium and S-Sulphur).

3.5. Optimization of Shatavarin IV content

The results of this study showed that soil nutrient management, specifically increasing or decreasing the quantities of sensitive elements like nitrogen and phosphorus in the soil, can enhance the content of Shatavarin IV. This was accomplished by altering the ANN model's representation of soil components like nitrogen and phosphorus, which have a significant impact on the Shatavarin IV content. In the developed ANN model, nitrogen level was increased from 144 to 175 kg/ha and phosphorus levels was increased from 43 to 55 kg/ha (Fig. 9). The Shatavarin IV content was increased to 0.300% after the sensitive factors in the produced ANN model were changed, which was higher than the Shatavarin IV content (0.245%) obtained from the initial ANN model.

The present optimization study shows that an increase in soil nitrogen and phosphorus content could exhibit a corresponding increase in the amount of Shatavarin IV which would therefore be helpful in formulating the fertilizers for good cultivation practice of *A. racemosus*. The optimal limits of nitrogen and phosphorus however need to be estimated precisely by field experiments.

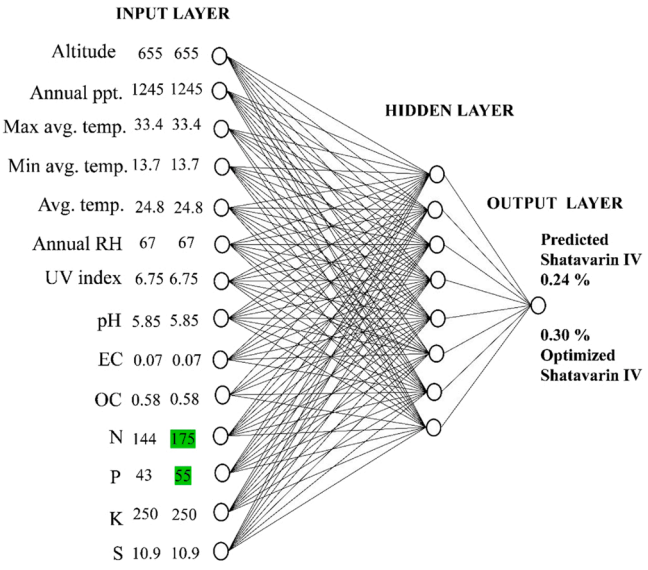

Fig. 9. Optimization of Shatavarin IV content by changing input parameters of the ANN model. (The highlighted sensitive factors were changed).

4. Conclusion

The developed ANN-MPL model with 14–8–1 architecture had shown efficient predictive ability with 90.740% efficiency at a new location. The sensitivity analysis revealed that the levels of nitrogen and phosphorus are largely responsible for the variation in the Shatavarin IV content and could be increased from 0.245% to 0.300% on dry weight basis by managing these sensitive factors in the developed model. It is seen from the study that the climatic factors have lower impact on the content of Shatavarin IV which need to be explored further. The soil nutrients like nitrogen and phosphorus play an important role in the biosynthesis of Shatavarin IV and the exact role need to be investigated further. Therefore, proper soil nutrient management programmes and selecting suitable cultivation site could produce high Shatavarin IV yielding *A. racemosus* for industrial uses in order to meet high demand. Further, the present study can be helpful in better understanding and establishing the molecular mechanism of how nitrogen and phosphorus affect the biosynthesis of Shatavarin IV and the precise role of nitrogen and phosphorus if defined would help to standardise their right amount of application in the field for better yield of Shatavarin IV in future.

Funding

This work is financially supported by Science and Engineering Research Board, Govt. of India (Grant No. EMR/2016/001802).

CRediT authorship contribution statement

Bibhuti Bhusan Champati, Bhuban Mohan Padhiari: Conceptualization, Formal analysis, Data curation, Writing – original draft. **Bibhuti Bhusan Champati, Asit Ray, Sudipta Jena and Ambika Sahoo**: Investigation. **Bibhuti Bhusan Champati, Bhuban Mohan Padhiari and Asit Ray:** Methodology. **Bibhuti Bhusan Champati, Asit Ray and Pradeep Kumar Naik**: Software. **Bibhuti Bhusan Champati, Sujata Mohanty and Jeetendranath Patnaik**: Validation. **Pratap Chandra Panda**: Supervision. **Sanghamitra Nayak**: Project administration, Funding acquisition, Writing – review & editing.

Declaration of Competing Interest

The authors declare that they have no known competing financial interests or personal relationships that could have appeared to influence the work reported in this paper.

Data availability

Data will be made available on request.

Acknowledgment

The authors would like to acknowledge the support and encouragement of Si, S.C., Dean, Centre of Biotechnology, and Nayak, M.R., President, Siksha 'O' Anusandhan (Deemed to be University).

References

Abdi-Khanghah, M., Bemani, A., Naserzadeh, Z., Zhang, Z., 2018. Prediction of solubility of N-alkanes in supercritical CO_2 using RBF-ANN and MLP-ANN. J. CO_2 Util. 25, 108–119. https://doi.org/10.1016/j.jcou.2018.03.008.

Akbar, A., Kuanar, A., Joshi, R.K., Sandeep, I.S., Mohanty, S., Naik, P.K., Mishra, A., Nayak, S., 2016. Development of prediction model and experimental validation in predicting the curcumin content of turmeric (*Curcuma longa* L.). Front. Plant Sci. 7, 1507. https://doi.org/10.3389/fpls.2016.01507.

Akbar, A., Kuanar, A., Patnaik, J., Mishra, A., Nayak, S., 2018. Application of artificial neural network modeling for optimization and prediction of essential oil yield in turmeric (*Curcuma longa* L.). Comput. Electron. Agric. 148, 160–178. https://doi.org/10.1016/j.compag.2018.03.002.

Alam, M.A., Naik, P.K., 2009. Impact of soil nutrients and environmental factors on podophyllotoxin content among 28 *Podophyllum hexandrum* populations of northwestern Himalayan region using linear and nonlinear approaches. Commun. Soil Sci. Plant Anal. 40, 2485–2504. https://doi.org/10.1080/00103620903111368.

Amedi, H.R., Baghban, A., Ahmadi, M.A., 2016. Evolving machine learning models to predict hydrogen sulfide solubility in the presence of various ionic liquids. J. Mol. Liq. 216, 411–422. https://doi.org/10.1016/j.molliq.2016.01.060.

Arya, R.H., Shincymol, V.V., Oommen, S.M., 2018. An insight to the pharmacognosy of shatavari (*Asparagus racemosus* willd.). Int. J. Ayur. Pharm. Res. 6, 49–52.

Benghanem, M., Mellit, A., 2010. Radial Basis Function Network-based prediction of global solar radiation data: Application for sizing of a standalone photovoltaic system at Al-Madinah. Saudi Arab. Energy 35, 3751–3762. https://doi.org/10.1016/j.energy.2010.05.024.

Bray, R.H., Kurtz, L.T., 1945. Determination of total, organic, and available forms of phosphorus in soils. Soil Sci. 59, 39–46.

Casalino, G., Facchini, F., Mortello, M., Mummolo, G., 2016. ANN modelling to optimize manufacturing processes: The case of laser welding. IFAC-Pap. 49, 378–383. https://doi.org/10.1016/j.ifacol.2016.07.634.

Champati, B.B., Padhiari, B.M., Ray, A., Halder, T., Jena, S., Sahoo, A., Kar, B., Kamila, P. K., Panda, P.C., Ghosh, B., Nayak, S., 2022. Application of a Multilayer Perceptron Artificial Neural Network for the Prediction and Optimization of the Andrographolide Content in *Andrographis paniculata*. Molecules 27, 2765. https://doi.org/10.3390/molecules27092765.

Chen, J., Xu, Y., Wei, G., Liao, S., Zhang, Y., Huang, W., Yuan, L., Wang, Y., 2015. Chemotypic and genetic diversity in *Epimedium sagittatum* from different geographical regions of China. Phytochem 116, 180–187. https://doi.org/10.1016/j.phytochem.2015.04.005.

Gaurav, A.K., Raju, D.V.S., Janakiram, T., Swaroop, K., Singh, B., Jain, R., Gopalakrishnan, S., 2014. Microclimate modification under different shade levels and its effect on the growth of *Dracaena fragrans*. J. Ornam. Hortic. 17, 12–17.

Ghorbani, M.A., Zadeh, H.A., Isazadeh, M., Terzi, O., 2016. A comparative study of artificial neural network (MLP, RBF) and support vector machine models for river flow prediction. Environ. Earth Sci. 75, 1–14.

Giri, A.K., Patel, R.K., Mahapatra, S.S., 2011. Artificial neural network (ANN) approach for modelling of arsenic (III) biosorption from aqueous solution by living cells of *Bacillus cereus* biomass. Chem. Engr. J. 178, 15–25. https://doi.org/10.1016/j.cej.2011.09.111.

Golovko, V., Savitsky, Y., Laopoulos, T., Sachenko, A., Grandinetti, L., 2000, Technique of learning rate estimation for efficient training of MLP, in: Proceedings of the IEEE-INNS-ENNS International Joint Conference on Neural Networks. IJCNN 2000. Neural Computing: New Challenges and Perspectives for the New Millennium. 1, 323–328. https://doi.org/10.1109/IJCNN.2000.857856.

Goyal, R.K., Singh, J., Lal, H., 2003. *Asparagus racemosus*-an update. Indian J. Med. Sci. 57, 408–414.

Haldar, S., Mohapatra, S., Singh, R., Katiyar, C.K., 2018. Quantitative evaluation of shatavarin IV by high-performance thin-layer chromatography and its isolation from *Asparagus racemosus* Willd. JPC-J. Planar Chromatogr. -Mod. TLC 31, 197–201. https://doi.org/10.1556/1006.2018.31.3.3.

Harpham, C., Dawson, C.W., Brown, M.R., 2004. A review of genetic algorithms applied to training radial basis function networks. Neural Comput. Appl. 13, 193–201. https://doi.org/10.1007/s00521-004-0404-5.

Hayes, P.Y., Jahidin, A.H., Lehmann, R., Penman, K., Kitching, W., De Voss, J.J., 2006. Structural revision of shatavarins I and IV, the major components from the roots of *Asparagus racemosus*. Tetrahedron Lett. 47, 6965–6969. https://doi.org/10.1016/j.tetlet.2006.07.121.

International Conference on Harmonization ICH, 2005, Vol. Q2. Geneva: ICH Secretariat; p. R1.

Jimeno-Sáez, P., Senent-Aparicio, J., Pérez-Sánchez, J., Pulido-Velazquez, D., 2018. A comparison of SWAT and ANN models for daily runoff simulation in different climatic zones of peninsular Spain. Water 10, 192. https://doi.org/10.3390/w10020192.

Joshi, R.K., 2016. *Asparagus racemosus* (Shatawari), phytoconstituents and medicinal importance, future source of economy by cultivation in Uttrakhand: A review. Inter. J. Herb. Med. 4, 18–21.

Kashaninejad, M., Dehghani, A.A., Kashiri, M., 2009. Modeling of wheat soaking using two artificial neural networks (MLP and RBF). J. Food engr 91, 602–607. https://doi.org/10.1016/j.jfoodeng.2008.10.012.

Kim, J.H., Chang, E.J., Oh, H.I., 2005. Saponin production in submerged adventitious root culture of *Panax ginseng* as affected by culture conditions and elicitors. Asia Pac. J. Mol. Biol. Biotech. 13, 87–91.

Le, L.T., Lee, G., Park, K.S., Kim, H., 2020. Neural network-based fuel consumption estimation for container ships in Korea. Marit. Policy Manag 47, 615–632. https://doi.org/10.1080/03088839.2020.1729437.

Liu, S., Zhong, J.J., 1998. Phosphate effect on production of ginseng saponin and polysaccharide by cell suspension cultures of *Panax ginseng* and *Panax quinquefolium*. Process Biochem 33, 69–74. https://doi.org/10.1016/S0032-9592(97)00064-2.

Majumdar, S., Gupta, S., Prajapati, S.K., Krishnamurthy, S., 2021. Neuro-nutraceutical potential of *Asparagus racemosus*: a review. Neurochem. Int. 145, 105013 https://doi.org/10.1016/j.neuint.2021.105013.

Mata, J., 2011. Interpretation of concrete dam behaviour with artificial neural network and multiple linear regression models. Engr. Struct. 33, 903–910. https://doi.org/10.1016/j.engstruct.2010.12.011.

Mellit, A., Kalogirou, S., 2008. Artificial intelligence techniques for photovoltaic applications: a review. Prog. Energy Comb. Sci. 34, 574–632. https://doi.org/10.1016/j.pecs.2008.01.001.

Mishra, J., Dash, A.K., Kumar, S., 2013. Hundred problems, one solution *Asparagus racemosus*. World J. Pharma. Res. 3, 201–211.

Mishra, T., 2016. Climate change and production of secondary metabolites in medicinal plants: a review. Int. J. Herb. Med. 4, 27–30.

Moore, B.D., Andrew, R.L., Külheim, C., Foley, W.J., 2014. Explaining intraspecific diversity in plant secondary metabolites in an ecological context. N. Phytol. 201, 733–750. https://doi.org/10.1111/nph.12526.

Muller, V., Lankes, C., Zimmermann, B.F., Noga, G., Hunsche, M., 2013. Centelloside accumulation in leaves of *Centella asiatica* is determined by resource partitioning between primary and secondary metabolism while influenced by supply levels of either nitrogen, phosphorus or potassium. J. Plant Physiol. 170, 1165–1175. https://doi.org/10.1016/j.jplph.2013.03.010.

Nell, M., Voetsch, M., Vierheilig, H., Steinkellner, S., Zitterl-Eglseer, K., Franz, C., Novak, J., 2009. Effect of phosphorus uptake on growth and secondary metabolites of garden sage (Salvia officinalis L.). J. Sci. Food Agric. 89, 1090–1096. https://doi.org/10.1002/jsfa.3561.

Nelson, D.A., Sommers, L., 1983. Total carbon, organic carbon, and organic matter. Methods Soil Anal.: Part 2 Chem. Microbiol. Prop. 9, 539–579.

Oludolapo, O.A., Jimoh, A.A., Kholopane, P.A., 2012. Comparing performance of MLP and RBF neural network models for predicting South Africa's energy consumption. J. Energy South. Afr. 23, 40–46.

Padhiari, B.M., Ray, A., Champati, B.B., Jena, S., Sahoo, A., Kuanar, A., Halder, T., Ghosh, B., Naik, P.K., Patnaik, J., Mohanty, S., 2022. Artificial neural network (ANN) model for prediction and optimization of bacoside A content in Bacopa monnieri: A statistical approach and experimental validation. Plant Biosyst. - Int. J. Deal. all Asp. Plant Biol. 3, 1–2. https://doi.org/10.1080/11263504.2022.2048278.

Page, A.L., Miller, R.H., Keeney, D.R., 1982. Methods of soil analysis, part 2: Chemical and microbiological properties. Madison WI: American Society of Agronomy. Soil Sci. Soc. Am. 595–624.

Ray, A., Halder, T., Jena, S., Sahoo, A., Ghosh, B., Mohanty, S., Mahapatra, N., Nayak, S., 2020. Application of artificial neural network (ANN) model for prediction and optimization of coronarin D content in *Hedychium coronarium*. Ind. Crops Prod. 146, 112186 https://doi.org/10.1016/j.indcrop.2020.112186.

Saran, P.L., Singh, S., Solanki, V.H., Kalariya, K.A., Meena, R.P., Patel, R.B., 2019. Impact of shade-net intensities on root yield and quality of *Asparagus racemosus*: A viable option as an intercrop. Ind. Crops Prod. 141, 111740 https://doi.org/10.1016/j.indcrop.2019.111740.

Saran, P.L., Singh, S., Solanki, V.H., Devi, G., Kansara, R.V., Manivel, P., 2020. Identification of potential accessions of *Asparagus racemosus* for root yield and shatavarin IV content. Heliyon 6, e05674. https://doi.org/10.1016/j.heliyon.2020.e05674.

Saran, P.L., Singh, S., Solanki, V., Choudhary, R., Manivel, P., 2021. Evaluation of *Asparagus adscendens* accessions for root yield and shatavarin IV content in India. Turkish J. Agric. Forestry 45, 475–483. https://doi.org/10.3906/tar-2006-42.

Sheikh, S.K., Unde, M.G., 2012. Short term load forecasting using ANN technique. Int. J. Eng. Sci. Emerg. Technol. 1, 97–107.

Smita, S.S., Raj Sammi, S., Laxman, T.S., Bhatta, R.S., Pandey, R., 2017. Shatavarin IV elicits lifespan extension and alleviates Parkinsonism in Caenorhabditis elegans. Free Radic. Res 51, 954–969. https://doi.org/10.1080/10715762.2017.1395419.

Subbiah, B., Asija, G.L., 1956. A rapid procedure for estimation of available nitrogen in soils. Curr. Sci. 25, 259–260.

Thakur, S., Kaurav, H., Chaudhary, G., 2021. Shatavari (Asparagus Racemosus)-The Best Female Reproductive Tonic. Int. J. Res. Rev. 8, 73–84. https://doi.org/10.52403/ijrr.20210511.

Tripathi, D.K., Singh, V.P., Chauhan, D.K., Prasad, S.M., Dubey, N.K., 2014. Role of macronutrients in plant growth and acclimation: recent advances and future prospective. Improv. Crops era Clim. Chang. 197–216. https://doi.org/10.1007/978-1-4614-8824-8_8.

Van Wyk, A.S., Prinsloo, G., 2020. Health, safety and quality concerns of plant-based traditional medicines and herbal remedies. South Afr. J. Bot. 133, 54–62. https://doi.org/10.1016/j.sajb.2020.06.031.

Venugopal, C.K., Mokashi, A.N., Jholgiker, P., 2008. Studies on comparative performance of patchouli (*Pogostemon patchouli* Benth.) under open and partial shade ecosystem. J. Med. Arom. Plant Sci. 30, 22–26.

Wei, W., Ye, C., Huang, H.C., Yang, M., Mei, X.Y., Du, F., He, X.H., Zhu, S.S., Liu, Y.X., 2020. Appropriate nitrogen application enhances saponin synthesis and growth mediated by optimizing root nutrient uptake ability. J. Ginseng Res 44, 627–636. https://doi.org/10.1016/j.jgr.2019.04.003.

Yang, L., Wen, K.S., Ruan, X., Zhao, Y.X., Wei, F., Wang, Q., 2018. Response of plant secondary metabolites to environmental factors. Molecules 23, 762. https://doi.org/10.3390/molecules23040762.

Yilmaz, I., Kaynar, O., 2011. Multiple regression, ANN (RBF, MLP) and ANFIS models for prediction of swell potential of clayey soils. Expert Syst. Appl. 38, 5958–5966.

Zare, M., Pourghasemi, H.R., Vafakhah, M., Pradhan, B., 2013. Landslide susceptibility mapping at Vaz Watershed (Iran) using an artificial neural network model: a comparison between multilayer perceptron (MLP) and radial basis function (RBF) algorithms. Arab. J. Geosci. 6, 2873–2888. https://doi.org/10.1007/s12517-012-0610-x.

Zhang, J.Y., Cun, Z., Wu, H.M., Chen, J.W., 2020. Integrated analysis on biochemical profiling and transcriptome revealed nitrogen-driven difference in accumulation of saponins in a medicinal plant *Panax notoginseng*. Plant Physiol. Biochem. 154, 564–580. https://doi.org/10.1016/j.plaphy.2020.06.049.

Zhang, T., Han, M., Yang, L., Han, Z., Cheng, L., Sun, Z., Yang, L., 2018. The effects of environmental factors on ginsenoside biosynthetic enzyme gene expression and saponin abundance. Molecules 24, 14. https://doi.org/10.3390/molecules24010014.

Zhong, J.J., Zhu, Q.X., 1995. Effect of initial phosphate concentration on cell growth and ginsenoside saponin production by suspended cultures of Panax notoginseng. Appl. Biochem. Biotech. 55, 241–247. https://doi.org/10.1007/BF02786863.